HAW
HAMBURG

BACHELORTHESIS
José Luis Roldán Rodríguez

Microprocessor controlled power supply and motor control board for an autonomous weather station

FACULTY OF COMPUTER SCIENCE AND ENGINEERING
Department of Information and Electrical Engineering

Fakultät Technik und Informatik
Department Informations- und Elektrotechnik

HAMBURG UNIVERSITY
OF APPLIED SCIENCES

Hochschule für Angewandte
Wissenschaften Hamburg

José Luis Roldán Rodríguez

Microprocessor controlled power supply and motor control board for an autonomous weather station

Bachelor Thesis based on the examination and study regulations
for the Bachelor of Engineering degree programme
Bachelor of Science Information Engineering
at the Department of Information and Electrical Engineering
of the Faculty of Engineering and Computer Science
of the University of Applied Sciences Hamburg
Supervising examiner: Prof. Dr. Lutz Leutelt
Second examiner: Prof. Dr. Martin Lapke

Day of delivery: 8. March 2024

José Luis Roldán Rodríguez

Title of Thesis

Microprocessor controlled power supply and motor control board for an autonomous weather station

Keywords

Weather station, TM4C1294NCPDT, TivaWare, EK-TM4C1294XL Launchpad, PCB, Microcontroller, Solar-panel

Abstract

This thesis aims to extend the development of the innovative autonomous solar-powered weather station project at Hamburg University of Applied Sciences. In doing so, it showcases the practical and theoretical knowledge acquired by students in the Faculty of Engineering and Computer Sciences; it also seeks to attract new talents to these fields. The emphasis of this study lies in the design and development of a power supply and motor control board for the weather station. The primary objective of this board is to optimize the solar energy capturing capabilities of the weather station by dynamically aligning the solar panel with the sun's position, utilizing the calculated azimuthal and elevation directions. In addition, this thesis incorporates power metering features and ensures integration with the existing hardware of the weather station.

José Luis Roldán Rodríguez

Thema der Arbeit

Mikroprozessorgesteuerte Stromversorgungs- und Motorsteuerungsplatine für eine autonome Wetterstation

Stichworte

Wetterstation, TM4C1294NCPDT, TivaWare, EK-TM4C1294XL Launchpad, Platine, Mikrocontroller, Solarpanel

Kurzzusammenfassung

Ziel dieser Arbeit ist es, das innovative Projekt einer autonomen, solarbetriebenen Wetterstation an der Hochschule für Angewandte Wissenschaften Hamburg weiterzuentwickeln. Dabei sollen die praktischen und theoretischen Kenntnisse der Studierenden der Fakultät für Ingenieurwissenschaften und Informatik aufgezeigt und neue Talente für diese Bereiche gewonnen werden.
Der Schwerpunkt dieser Studie liegt auf dem Entwurf und der Entwicklung einer innovativen Stromversorgungs- und Motorsteuerungsplatine für die Wetterstation. Das Hauptziel dieser Platine ist es, die Optimierung der Solarenergieerfassung durch die dynamische Ausrichtung des Solarpanels auf den Sonnenstand unter Verwendung der berechneten Azimut- und Elevationsrichtungen zu ermöglichen. Darüber hinaus beinhaltet diese Arbeit Funktionen zur Leistungsmessung und gewährleistet die Integration mit der bestehenden Hardware der Wetterstation.

Contents

List of Figures

List of Tables

1 Introduction

1.1 Motivation

In this modern era, a latent yet often overlooked problem is the management of energy consumption. As the transition from an analogue to a digital world occurs, our daily lives increasingly depend on devices powered by microcontrollers and computers. These devices, designed for convenience and efficiency, often prioritize speed over energy optimization, leading to excessive power consumption. This issue is aggravated as more powerful resources are developed, overshadowing the need for energy management. Thus, the importance of autonomous systems in the industry often leads to new perspectives. In today's rapidly digitalizing world, the efficient management of energy consumption emerges as a critical yet often underestimated challenge. The shift from analogue to digital has significantly increased our reliance on microcontroller-powered devices and computers, which, while designed for convenience and efficiency, frequently prioritize performance at the expense of energy conservation. This trend is exacerbated by the continuous development of more powerful technologies, which can overshadow the pressing need for effective energy management strategies. This thesis emphasizes the crucial role of autonomous systems in addressing these challenges, offering new perspectives for sustainable industry practices. It specifically explores the potential of an autonomous weather station, highlighting the critical issue of limited power resources and the station's importance for reliable meteorological data collection in remote areas. The central objective is to design and implement a microprocessor-controlled power supply and motor control board that maximizes solar panel efficiency through intelligent positioning, thereby optimizing resource utilization.

Specifically, the project involves creating a system that dynamically adjusts the solar panel's direction using two motors, ensuring optimal sun exposure. This thesis comprehensively covers the development of the electrical circuit and printed circuit board for both the power supply and motor control system. The designed system will seamlessly integrate with an existing microcontroller and sensor board. This integration will not only control the solar panel motors and read data from various weather sensors but also measure power consumption.

The primary goal of the "Weather Station" project is to establish a functional weather station at HAW Hamburg, demonstrating the real-world applications of the Electrical and Information Technology program to both future and current students, thereby promoting interest in enrollment. While this thesis contributes significantly to the development of the weather station, it's important to note that the project will not reach full completion.

1.2 Previous Work

The weather station project at HAW Hamburg has evolved significantly over the years, originating from a Sensor technology (Sensortechnik) master course within the Department of Information and Electrical Engineering. Initially designed as a group project aimed at developing solar-powered weather stations, it culminated with the submission of a station and a report, highlighting the hardware and software selection of the system. From these efforts, two stations remained at the university, though neither were fully operational weather stations. Due to technological advancements and physical deterioration over time, the components of these stations, developed in 2017, have become outdated and incompatible with newer systems.

Therefore, the revision and reconstruction of the weather station was initiated. The base for this project was established in the bachelor's thesis from Hasanova [17], a student of Information Engineering at the HAW. Hasanova's thesis focused on setting wireless communication, particularly the design and implementation of Wi-Fi and Bluetooth connectivity. These communication techniques enable the transmission of data to a mobile device via Bluetooth and to a web server via Wi-Fi enabling real-time data to be acquired and graphically displayed on the server's website. Additionally, key decisions essential for the project's progression were made, such as choosing the microcontroller that serves as the central control unit of the weather station.

Following the foundational contributions of [17], a student from the Department of Electrical Engineering and Information Technology (Elektrotechnik und Informationstechnik) took over the project. Westermann's bachelor thesis [37] concentrated on exploring specific hardware and sensors required for collecting measurements, and placing them on a board. Utilizing the existing chassis from a previous team, he integrated key components like the photovoltaic panel, sensors, and motors onto a rotatable turntable. This design can be seen in Figure 1.1.

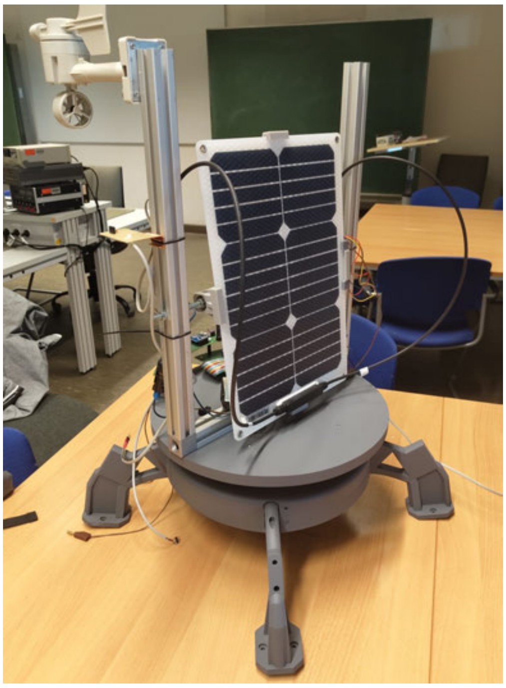

(a) Weather Station Front

(b) Weather Station Back

Figure 1.1: Previous Weather Station setup [37]

During the last update of the project, the university suffered a Cyberattack, resulting in the loss of information from the cloud storage. Some previous data was lost but the main source code for the project created by Hasanova and Westermann was recovered.

2 Fundamentals

2.1 Microcontroller

Microcontrollers are Integrated Circuits (ICs) designed to control a specific process in an embedded system [16]. A microcontroller consists of three main components: a processor, also known as the Central Processing Unit (CPU), responsible for computation and command execution; memory, divided into non-volatile and volatile types; and peripherals, which include input/output ports. Unlike microprocessors, which require external components to function, microcontrollers are designed for applications that require direct control of physical operations through electronic signals [16].
The primary advantage of microcontrollers is their ability to perform real-time operations with minimal power consumption and at a low cost. This makes them ideal for applications where energy efficiency is crucial, such as in automotive electronics, home appliances, medical devices, and various consumer electronics that require efficient control of physical operations.

Microcontrollers range considerably in terms of processing power, memory size, and range of peripherals. They can be programmed using various programming languages, with C and assembly language [36] being the most common. These are low-level languages, making it easier to interact with the hardware.

The Arduino platform is the most widely recognized microcontroller for personal projects, supported by a wide range of resources such as books, articles, blogs, and online tutorials [6]. However, for this project, a Tiva microcontroller was chosen due to its superior performance, advanced peripherals, and energy efficiency. This decision was supported by a comprehensive introduction to the Tiva microcontroller within the bachelor program.

2.1.1 Tiva EK-TM4C1294XL LaunchPad

For the weather station project, the TI Launchpad (EK-TM4C1294XL) was selected. The TI Launchpad is an evaluation board that incorporates the TM4C1294NCPDT microcontroller [33] from Texas Instruments.

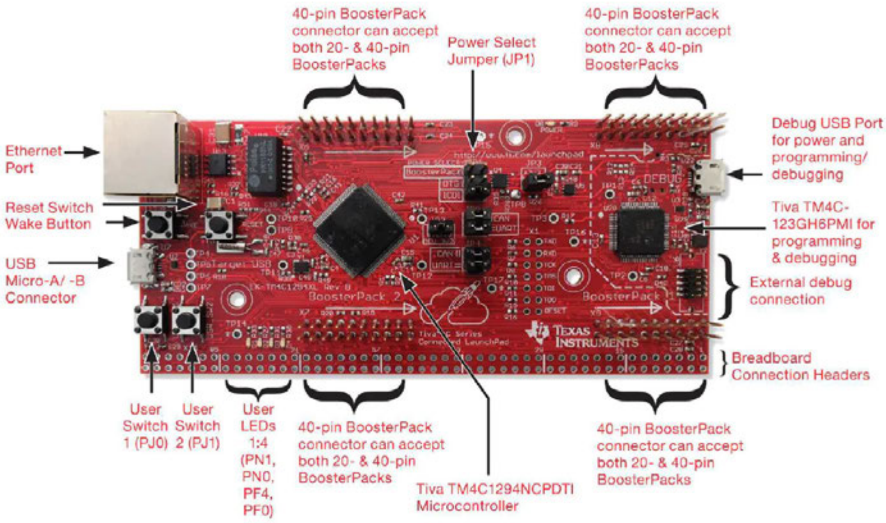

Figure 2.1: TI Launchpad extracted from [23].

This particular microcontroller is developed around the ARM Cortex M4 processor core, featuring an onboard debug interface to facilitate both programming and debugging activities. The board is comprehensively equipped with all the required external components, such as a power supply and ports for USB and Ethernet connectivity, enabling straightforward interfacing with various devices. It also incorporates LEDs, switches, and BoosterPack connectors, simplifying the process of establishing General Purpose Input/Output (GPIO) connections. For software development on the Launchpad, the environment Code Composer Studio (CCS) is available. CCS enhances the development experience by providing robust communication with a computer and a comprehensive library of functions that aid in the control and initialization of peripheral components, as well as in register manipulation.

2.2 Voltage Converter

Voltage converters are vital elements in embedded systems, as components may require different voltage levels from a single power source. These devices help to ensure stability, prolong the life span and increase efficiency of electronic circuits, especially in battery-powered applications where power efficiency is central.

There are two primary types of voltage converters: linear voltage regulators and switching voltage converters. Linear regulators offer simplicity and low noise output but are less efficient compared to their switching converters. Switching voltage converters, on the other hand, offer higher efficiency, especially in applications where the difference between input and output voltages is significant.

Switching voltage converters, also known as Switch-Mode Power Supplies (SMPS), operate with a high-frequency switching technique to convert electrical power efficiently. Unlike linear regulators that dissipate extra power as heat, similar to voltage dividers, SMPSs transfer energy via an inductor placed at the output to smooth the signal, facilitating the generation of a consistent voltage with minimal loss significantly improving power efficiency. The core principle of switching voltage converters lies in the rapid toggling of the input power, controlling the on-state and off-state durations, known as the duty cycle, to produce the desired output voltage. A control circuit dynamically adjusts this duty cycle in response to variations in input voltage or load conditions, ensuring the output voltage remains stable [18].

Switching voltage converters are highly efficient, achieving over 90% efficiency under optimal conditions [11], which is crucial for extending battery life in portable devices. They offer versatile output voltage ranges, both step-up and step-down, enhancing their utility in power management. However, they pose challenges such as Electromagnetic Interference (EMI) due to high-frequency switching, requiring a careful layout, filtering, and shielding to ensure the reliability of sensitive signals.

2.3 Hall Sensor

Hall sensors are based on the Hall effect principle [15]. Discovered in 1879 by Edwin Hall, the Hall effect involves voltage generation across a conductor with current, under a perpendicular magnetic field. This voltage, directly proportional to the magnetic field's intensity, enables contactless detection of magnetic fields by Hall sensors. This phenomenon is utilized in Hall sensors to detect magnetic field strength.

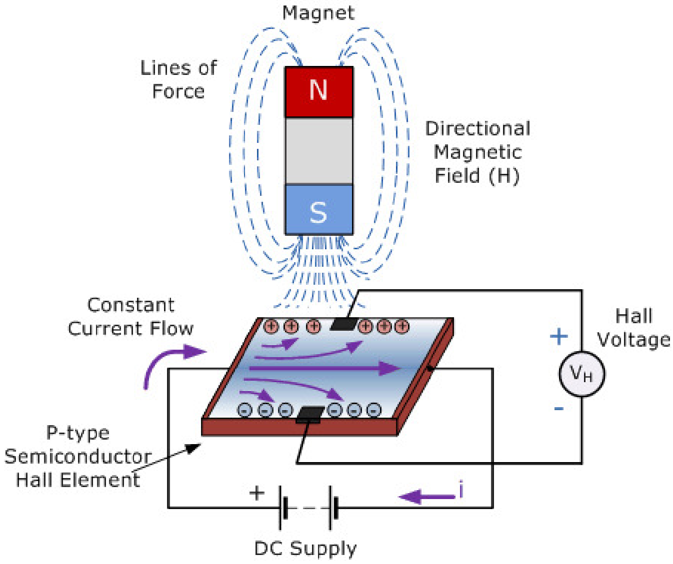

Figure 2.2: Hall effect principle extracted from [31]

The operation of a Hall sensor can be summarised as passing a constant current through the sensor, and when exposed to a magnetic field, a voltage difference is generated across it. This voltage difference, proportional to the magnetic field's intensity, is then measured typically with an Analogue to Digital Converter (ADC).

Hall sensors offer the advantages of contactless operation, long-term reliability, and the ability to detect a wide range of magnetic fields, making them indispensable in various applications, from automotive to consumer electronics.

2.4 DC Motor and Motor Driver

Direct Current (DC) motors convert direct current electrical energy into mechanical energy, widely utilized across various applications from household appliances to industrial machinery [10]. Key components of a DC motor include:

- **Stator**: The stationary part that produces a magnetic field, either through a magnet or windings.

- **Rotor (Armature)**: The rotating part within the magnetic field.
- **Commutator**: A rotary switch inverting current direction in the armature windings to maintain rotation.
- **Brushes**: Conductive contacts transferring electricity to the armature via the commutator.

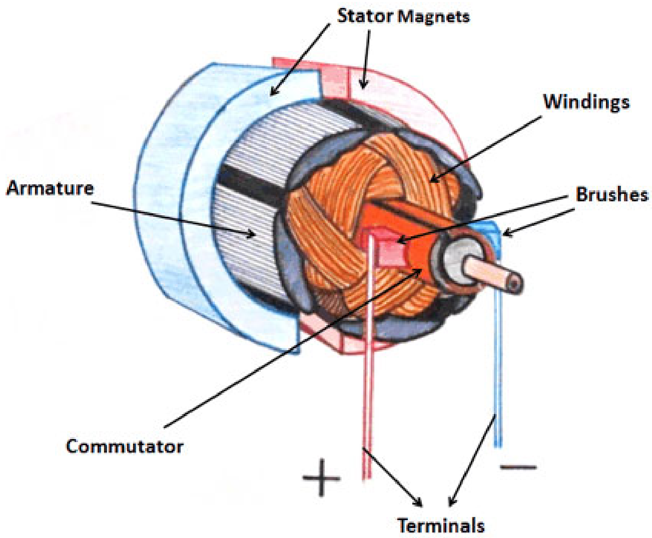

Figure 2.3: Section view of a DC motor. Extracted from [29]

Operating on the Lorentz force principle, with direction determined by Fleming's left-hand rule [10], DC motors are essential for their simplicity, reliability, and control ease.

DC motors are categorized by their magnetic field generation method into:

- **Brushed DC Motors**: These motors rely on brushes and a commutator to create movement. Known for their straightforward design and cost-effectiveness, they do, however, require periodic maintenance to address brush wear.
- **Brushless DC Motors (BLDC)**: BLDC motors utilize an external electronic controller for phase management instead of brushes. This approach improves efficiency, enhances reliability, and significantly extends operational lifespan.

Motor drivers are crucial for connecting microcontrollers and motors, as well as, amplifying signals to control motor speed, direction, and torque. Speed is regulated via Pulse Width Modulation (PWM) for precise adjustments without losing torque, while direction and torque are managed by changing voltage polarity and current flow, respectively. An additional feature the motor driver offers is protection mechanisms like overcurrent protection, thermal shutdown, and under-voltage lockout, crucial for the motor and driver longevity.

2.5 Solar Position Algorithm

Understanding the position of the Sun is crucial for optimizing the yield of power from the solar panel. Research indicates that stationary solar panels can produce up to 30-40% less energy throughout the day compared to those equipped with a tracking system [26]. Thus the importance of tracking the star with the photovoltaic panel cannot be overstated.

To dynamically position a solar panel three methods can be applied. The simplest approach would be to measure real-time power output to find the optimal position, which could only be feasible without any sensor data or time reference, being highly inefficient and equivalent to using brute force. A second approach would be to utilize a predefined movement based on time, which is suitable for systems with lower computational capabilities as it does not require calculating the sun's position every time. This method, however, does not yield maximum efficiency for locations far from the Equator due to Earth's axial tilt affecting sun exposure.

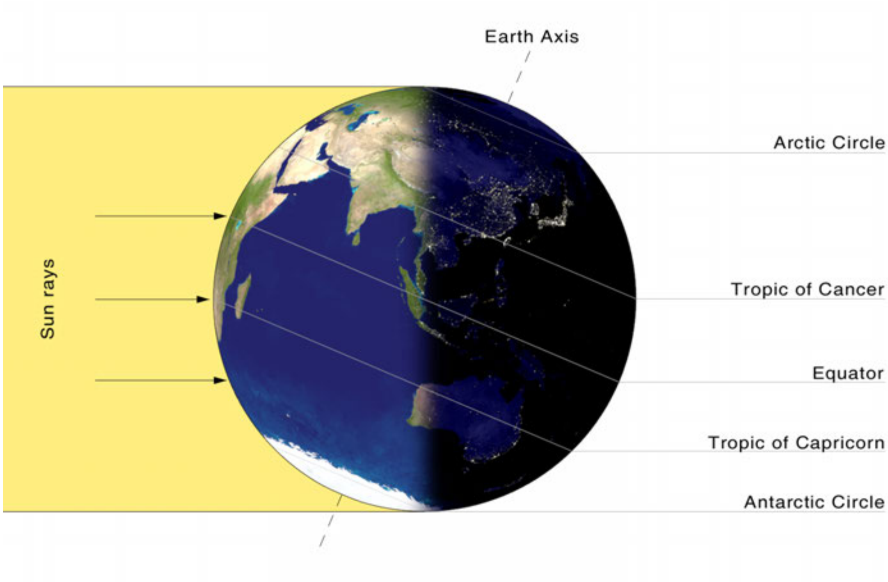

Figure 2.4: Earth [19]

The final approach explored the utilization of the Solar Position Algorithm (SPA) for Solar Radiation Applications from the National Renewable Energy Laboratory (NREL) [24]. This is an industry standard approach, noted for its precision, having undergone rigorous validation processes against other solar positioning models. The SPA calculates the Sun's position by considering its Zenith and Azimuth angles, tied to the stable geographic North Pole. This process, illustrated in 2.5, considers Earth's elliptical orbit, axial tilt, and equinox precession for optimal solar panel positioning. SPA's methodology, achieving ±0.0003% precision by considering the sun's position and the light interaction with Earth's atmosphere, incorporates complex astronomical data into its calculations, like timezone, longitude, latitude, and specific atmospheric conditions, essential for maximizing solar energy capture.

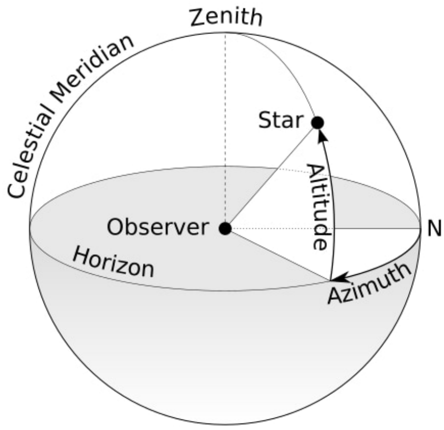

Figure 2.5: Azimuth and altitude [38]

SPA involves complex transformations of astronomical coordinates and detailed computations like the Julian date, solar declination, equation of time, and solar hour angle, requiring accurate astronomical data and constants. For a detailed understanding of these complex processes, the paper cited offers a complete analysis of the SPA principles [24].

3 Requirements

The main focus of this chapter is the fundamental and specific requirements necessary for the design and development of the microprocessor-controlled power supply and motor control board for an autonomous weather station. These requirements are divided into hardware and software components to provide a comprehensive understanding of the system architecture. The hardware requirements focus on the physical components and functionalities, such as motor control and energy measurement, vital for the operation of the weather station. The software requirements emphasize the system logic, including algorithms for solar panel orientation and energy management. This systematic approach ensures a meticulous and detailed foundation for developing a robust and efficient weather station.

3.1 Requirements Inception

Requirements inception is an indispensable element of the requirements chapter, emphasizing the processes and methods for gathering, analyzing, and defining specific needs for the microprocessor-controlled power supply and motor control board. This phase is essential for accurately determining and refining the system functionality to meet user expectations.

3.1.1 Stakeholder Identification

The stakeholder scheme for the weather station project is required for the demonstration of its objectives, which, as previously mentioned, is to showcase the practical utility of Electrical and Information Engineering studies. This project is not just an academic exercise; it is strategically positioned to spark interest. Stakeholders are primarily divided into two key groups:

1. **Educational Beneficiaries:** This group consists of individuals who stand to gain educational value from the interaction with the weather station. They include:
   - Current and future students who can learn from and engage with the station.
   - Faculty members who may utilize the station as a teaching aid in courses.
   - Visiting scholars or guests who are shown the capabilities of the station during tours or presentations.
2. **Technical Contributors:** This group comprises individuals who will contribute to the technical aspects of the weather station. They are likely to be involved in the design, implementation, and maintenance phases. This group includes:
   - Technical staff responsible for the operational integrity of the station.
   - Students and researchers who contribute to the ongoing development and enhancement of the station.
   - Collaborators from other departments or institutions who provide technical expertise.

3.1.2 Requirement Derivation

In the foundational work specified by [17], the requirements for a fully equipped weather station have been established. To avoid redundancy, in this thesis the focus will be exclusively on the specific requirements related to the microprocessor-controlled power supply and motor control board.
The requirements have been meticulously derived from a combination of investigative research and the unique needs presented by the current project phase. Furthermore, these requirements have been refined through discussions with key project stakeholders, the project leader and the supervising professor, who serves as the primary academic advisors and contributors to the project. The detailed requirements are categorized as follows:

- **Power Management:**
  – Efficiently charge an accumulator using both the photovoltaic panel and external power sources.

  - Transform voltage levels to meet the operational levels of the Tiva microcontroller.
  - Monitor and measure critical current flows within the station to ensure optimal performance.
  - Implement strategies for minimizing power consumption without compromising station functionality.

- **Solar Panel Movement:**
  - Enable independent control of dual motors for precise positioning.
  - Implement algorithms to accurately calculate the Sun's position throughout the day.
  - Adjust the solar panel orientation to maximize exposure to sunlight based on calculated positions.

- **Documentation:**
  - Produce comprehensive documentation detailing operational instructions for future users and maintainers of the weather station.

3.2 Requirements Specification

Once the requirements have been outlined, a detailed overview of the essential hardware and software requirements for the autonomous weather station project were defined. This includes a detailed examination of both Functional Requirement (F) and Non-Functional Requirement (NF) aspects.

3.2.1 Hardware

This section introduces the hardware requirements specification, focusing particularly on the motor functionality. It outlines the critical components needed to ensure comprehensive operational capabilities. The accompanying table categorizes each requirement by its unique ID, distinguishes between F and NF types, and provides a detailed description.

ID	Type	Requirement
Power Management		
1	F	The hardware should enable charging the accumulator through two methods: solar and external.
2	F	The hardware must support measuring the current from the solar panel.
3	F	The power management system should be able to sustain the supply board, microcontroller board and sensor board.
4	F	Transform voltage levels to meet the operational needs of the Tiva microcontroller and sensors.
5	NF	Implement strategies for minimizing power consumption without compromising station functionality.
Solar Panel Movement		
6	F	The weather station must be able to turn 360 degrees.
7	F	Independent control of both motors is required.
8	F	The system should be capable of operating the motors in both directions.
9	NF	The specified motors and solar panels must be compatible and operational within the system design constraints.
Documentation		
10	NF	Produce comprehensive documentation including operational instructions for future users and maintainers.
11	NF	Detailed documentation must include a table of pins, specifying the exact locations, types, and specific functions of all pin connectors, enhancing modularity and troubleshooting.
General Requirements		
12	NF	External connectors must be securely attached and protected to ensure system reliability and prevent wire disconnections.
13	NF	The design must preserve the board shape to integrate with existing systems.
14	NF	Sufficient space must be allocated for the battery to ensure fit and ease of installation.
15	NF	The system must be capable of reading the state of a snap action switch to provide operational status.
16	NF	Offers an intuitive and user-friendly interface for users with minimal technical expertise.

Table 3.1: Hardware Requirements Specification

3.2.2 Software

This section elaborates on the software requirements, underlining solar adjustment functionalities. Similar to Table 3.1, the subsequent table organizes these requirements, providing a clear framework for understanding the software's pivotal role in the project's success.

ID	Type	Requirement
		Power Management
17	F	Develop periodic measures to sample the current readings and store them.
18	NF	Create efficient and optimised functions to minimise energy consumption.
		Solar Panel Movement
19	F	Develop and implement the solar formula to keep track of the sun's position at any time.
20	F	Software should control motor speed to prevent overheating of motor drivers.
21	F	Software shall adjust the solar panel orientation to optimize sunlight exposure, using calculated positions, with features for manual override and real-time tracking.
22	F	Engineer software for independent control of dual motors and implement interrupt functionality for the snap action switch to prevent the panel from exceeding boundaries.
		Documentation and Integration
23	NF	Software architecture should work with previous code, ensuring the correct functioning of the whole station
24	NF	Provide detailed documentation on software architecture, API interfaces, and integration guidelines, offering a comprehensive guide for developers and maintainers.
25	NF	Offer an intuitive and user-friendly interface for users with minimal technical expertise.

Table 3.2: Streamlined Software Requirements for Autonomous Weather Station

4 Concept

This chapter presents the Concept Plan of the thesis, focusing on the selection of hardware modules and the development of the software design concept. It connects the theoretical requirements from the previous chapter with practical choices, explaining the motivation behind selecting specific hardware and outlining the integrated software design.

4.1 Hardware

The Hardware, standing as an integral part of the Concept Plan, focuses on the meticulous selection and integration of essential components that underpin the functionality of the weather station project. It links together the theoretical groundwork established in previous discussions with practical component choices. This section not only summarises the specifications and roles of chosen hardware, such as voltage regulators, solar chargers, and motor controllers but also emphasizes their contribution towards a cohesive and efficient system design. Through a detailed examination of the requirements, the components needed for this segment were delineated. These include:

- Voltage regulator
- Solar Charger
- External Charger
- Accumulator
- Motors for solar panel alignment
- Motor controller
- Current measurement

- Solar Panel Position Measurement
- Board Design

4.1.1 Previous Connections

Previous to the selection of components, one should take into account the constraints, in this case, the available connection pins; as highlighted in the requirements analysis, providing full integration with previous components is crucial. In line with [37], a variety of jumper connections have been utilized, facilitating a range of connections from power supplies (5V, 3.3V, and GND) to digital and analogue inputs and outputs. The table below specifies the Standard Function of these digital and analogue ports.

Port	Standard Function
PA4	Aout
PA5	Aout
PD4	GPIO
PD5	Ain
PE1	Ain
PE2	Ain
PF1	PWM
PF2	PWM
PH0	GPIO
PH1	GPIO
PL0	GPIO
PL1	GPIO
PL2	GPIO
PL3	GPIO
PN2	GPIO
PN3	GPIO
PN4	I2C SDA
PN5	I2C SCL
PP0	UART RX
PP1	UART TX
PP2	GPIO
PP4	GPIO
PQ0	SPI CLK
PQ2	SPI MOSI
PQ3	SPI MISO

Table 4.1: Ports and Their Standard Functions

4.1.2 Voltage Regulator

The voltage regulator is a key component for the weather Station project to function, as the TIVA microcontroller and most of the sensors can not handle 12V directly from the accumulator. That's why an adequate method to reduce the voltage is needed. The criteria for the component selected was the most efficient for the specific application, as the weather station must not draw excessive amounts of current.

Param/Model	Vout	Iout	Efficiency	Type	Key Feature	Price
LM2673SX-5.0/NOPB	5 V	3 A	High	Switching	High efficiency	4.93€
L7805CV	5 V	1.5 A	Low	Linear	Thermal Protection	0.64€
LM2940LD-5.0/NOPB	5 V	1 A	Medium	Linear	Low Dropout	2.02€
LM1086IT-5.0/NOPB	5 V	1.5 A	Medium	Linear	Current Protection	2.11€
TPS54360	Adj	3.5 A	High	Switching	Thermal Shutdown	4.33€
MP2393GTL-Z	Adj	3 A	High	Switching	Sync. Rectification	1.47€
LM2593HVT-ADJ/NOPB	Adj	3 A	High	Switching	Adjustable Output	6.27€

Table 4.2: Comparison Table for Voltage Regulators. Prices extracted from [2].

Based on the comprehensive comparison and analysis of various voltage regulators seen in Table 5.2, the LM2673SX-5.0/NOPB has been selected as the best-suited solution for this project, based on these key factors:

- **High Efficiency**: Ensures minimal energy waste from the battery, crucial for extending operational time.
- **Adequate Current Capacity**: With a 3A output, it comfortably supports the maximum peak current requirement of 1A from the microcontroller described in the datasheet of the TIVA TM4C1294 [33], ensuring reliable operation.
- **Advanced Protection**: Features like the limiting current pin provide crucial overcurrent protection, addressing the absence of such safety measures when power is supplied through the Booster Pack.
- **Superior to Alternatives**: Outperforms linear regulators by minimizing power loss, and enhancing energy efficiency.

The LM2673SX-5.0/NOPB's efficiency, capability, and protection features make it the best-suited option for the weather station, aligning with the project's criteria for an effective voltage regulation solution.

4.1.3 Solar Charger

In the previously mentioned master program project, it was decided to use the solar charger (SOLAR-Laderegler 4A Typ 18123). This component is characterized by the following specifications:

- Nominal voltage: 12/24V
- Charging and Load Current: Up to 4A
- Self-Consumption: 1.5 mA
- Overcharge Protection: Moderates charge flow to prevent battery overcharging.

Upon further evaluation and consultation with the laboratory specialist, this charger was confirmed as the ideal choice for the project, with its focus on energy efficiency and waste reduction. Its overcharge protection is particularly valued for safeguarding the accumulator's longevity and operational safety.

4.1.4 External Charger

The educational objective of the weather station introduces challenges with the accumulator, particularly when stored for indefinite periods without solar recharging, leading to potential accumulator drain. To prevent this situation from happening, an external charging port was integrated. Connected to the previously mentioned "Solar Charger" with a 12V power supply, a setup that includes a protective measure against reverse current damaging the solar panel must be implemented. A Schottky diode, specifically the SK32 [13], with 20V Maximum Repetitive Reverse Voltage (VRRM) and 3A Maximum Forward Current (IF(AV)), was selected for its efficacy in preventing reverse current flow, thereby ensuring the solar panel protection while maintaining the accumulator charge.

4.1.5 Accumulator

For the current project, which primarily serves demonstration purposes and is not intended for continuous outdoor deployment, the accumulator choice is less critical. The selected VOLTCRAFT CP1212, with a capacity of 1.2 Ah, is considered sufficient as it is expected to be charged before each exhibition. Moreover, the moderate energy requirements for moving the solar panel actuators, which do not need to operate at maximum power, align with the chosen battery capacity. The compact dimensions of the CP1212 are ideal, allowing it to be mounted alongside the PCB without occupying excessive space.

Should the project scope change to a continuously operating weather station, a larger capacity battery would be recommended to accommodate prolonged run times, multiple recharge cycles, and slower degradation.

Model	Price (€)	Capacity (Ah)	Type	Dimensions (WxHxD)
VOLTCRAFT CP1212	9.24	1.2	AGM	97x58x43 mm
VOLTCRAFT CP1223	17.78	2.3	AGM	178x67x35 mm
VMAXTANKS Vmax857	105.85	35	AGM	196x155x127 mm
Offgridtec c20	219.9	150	Gel	486x171x243 mm
Mighty Max ML5-12	27	5	SLA	70x91x106.7 mm

Table 4.3: Comparison Table of Different Accumulator Models. Prices extracted from [2] & [1].

In the end, the VOLTCRAFT CP1212 was chosen for its balance between capacity, dimensions, and cost, adequately meeting the project requirements for demonstration purposes.

4.1.6 Motors for Solar Panel Alignment

In alignment with principles of sustainability and efficiency, the decision to recycle Modelcraft RB350600-0A101R motors stands as proof of the commitment to resource optimization. These motors, previously selected by master course students, have been selected due to their fitting specifications, which include:

- Operating voltage: 12 V/DC
- Speed under load: 9 rpm
- Max gear load: 18Kg/cm

These specifications ensure seamless integration with existing power supply configurations, offer the necessary mechanical output without compromising performance and provide substantial torque to handle anticipated loads from the gears with reliability and stability.

4.1.7 Motor Controller

The motor driver module stands as a fundamental pilon in the design of the board, with a focused methodology aimed at preventing overheating, minimizing power consumption, and incorporating built-in protection mechanisms. Given the outdated nature of the motor driver previously in use, extensive market research was undertaken. The findings from this analysis are presented in Table 4.4, which compares various motor controllers based on price, voltage range, maximum current, type of output configuration, and key specifications.

Model	Price	Range(V)	I max	Type	Key Specifications
DRV8833	4.9€	2.7-10.8	1.5A	Dual-H	Dual channel, thermal shutdown
L298N	2.65€	4.5-35	2A	Dual-H	High current, large heatsink
L293D	7.92€	4.5-36	0.6A	Dual-H	Built-in diodes, overheating protection
TB6612FNG	13.95€	2.5-13.5	1.2A	Dual-H	High efficiency, low standby current
DRV8871	2.54€	6.5-45	3.6A	Single-H	Current control, low power sleep mode
SN754410NE	2.73€	4.5-36	1A	Quadruple Half-H	4 driver channels, can be paralleled for higher current
DRV8231-DDAR	0.79€	4-33	3.7A	Single-H	PWM control, low power sleep mode, Integrated protection features
VNH5019	9.95€	5.5-24	12A	Dual-H	Robust high-current driver, current sensing
A4953	4.10€	8-40	3.5A	Dual-H	PWM current limiting

Table 4.4: Comparison Table of Motor Controllers. Prices extracted from [2].

Upon examination and consultation with the laboratory specialist, the DRV8231DDAR was identified as the most suitable choice, particularly the DDAR variant over the DSGR version. The DDAR is preferred due to its 8-SO PowerPad packaging, contrasting with the DSGR's 8-WSON (Very Very Thin Small Outline No Lead) packaging. The latter, while more compact, was expected to introduce challenges related to thermal management and soldering difficulties due to its minimal footprint and lack of lead pins. The DRV8231DDAR was chosen for several reasons. It offers an efficient low-power sleep mode, aligning with the operational requirements where motor activity is periodic. Furthermore, its design facilitates heat redirection to an external resistor, thereby reducing thermal accumulation within the component. This characteristic is critical for ensuring the reliability and longevity of the motor driver under variable operational conditions.

A challenge was encountered due to the limited availability of Pulse Width Modulation (PWM) generator ports on the microcontroller board, as referenced in Table 4.1 with only 2 PWM ports. The DRV8231 motor driver offers a practical solution to this issue by enabling the control of one input port for advancing the motor and another for reversing it, without necessitating simultaneous drive of both input ports. Consequently, a standard multiplexer, specifically one compatible with High-Speed CMOS technology (HCT) to accommodate the 3.3V logic levels from the microcontroller, was employed. This multiplexer facilitates the dynamic switching of both motor directions, seamlessly integrating with the microcontroller output capabilities.

4.1.8 Current Measurement

The design and implementation of the project control and monitoring frameworks demand the incorporation of accurate current measurement functionalities. To identify the most suitable current sensing solution, a selection process was undertaken, examining a range of devices based on their technical specifications and cost-effectiveness. The table below presents a list of current sensors, highlighting their key features and output types to facilitate an informed decision.

Device Model	Price	Output Type	Key Specifications
ACS712ELCTR	3.63€	Analog Voltage	Hall-effect sensor, 5A nominal measurement range, 66mV/A sensitivity
INA219	2.78€	Digital I2C	High-side current and voltage monitor with I2C interface, 0-26V bus voltage range
ACS770ECB	9.29€	Analog Voltage	Hall-effect sensor, 200A nominal measurement range, high accuracy
AD8217	2.7€	Analog Voltage	Zero-drift, bi-directional current shunt monitor
SS49E	3.8€	Analog Voltage	Linear Hall-effect sensor, operates from 2.7V to 6.5V supply
MAX4172ESA	5.87€	Analog Voltage	High-side current-sense amplifier, operates from a 2.7V to 5.5V supply
LTC4151IMS	8.38€	Digital I2C	High-side current and voltage monitor with I2C interface

Table 4.5: Comparison Table of Current Monitors. Prices extracted from [2].

After careful consideration, the ACS712ELCTR was chosen for its accuracy, cost-effectiveness, and reliability. This Hall Effect sensor enables non-invasive, precise current measurements, crucial for the project. It detects a wide range of currents without interfering with the circuit functionality. Additionally, its galvanic isolation feature guards against electrical disturbances, ensuring the safety and integrity of the data collection process and the electrical systems of the Tiva microcontroller.

4.1.9 Solar Panel Position Measurement

Achieving the optimal orientation of solar panels towards the sun requires precise knowledge of the photovoltaic current positioning. The system utilizes two key measurements to determine this positioning:

Direction Measurement

To determine the solar panel azimuthal direction, the system incorporates the "hmc5883l" compass sensor, a component previously integrated into the sensor board [37]. This sensor calculates the facing direction of the panel by detecting the strength and direction of Earth's magnetic fields. Continued functionality and compatibility with the system requirements were chosen as the main direction measurement device.

Angle Measurement

The method chosen for measuring the tilt angle of the solar panel was primarily influenced by the existing snap action switches, positioned at 0 and 90 degrees, to indicate the panel's horizontal and vertical orientations, respectively. This choice was driven by the method's simplicity, cost-effectiveness, and the ability to integrate seamlessly with the existing system infrastructure, thus avoiding the need for substantial modifications.

By utilizing a constant motor rate to drive the panel between these predefined positions, the system can precisely calculate the tilt angle based on the duration of movement and the motor speed.

Together, these measurement techniques form a comprehensive approach for adjusting the solar panel orientation, ensuring maximum exposure to sunlight and optimizing the efficiency of the solar tracking system. The strategic use of existing technologies within this setup highlights a practical and resourceful engineering solution.

4.1.10 Board Design

The PCB design, pivotal for integrating the project hardware components, was accomplished using Eagle PCB design software [7]. Selected for its compatibility with existing designs to ensure symmetry with previous boards, Eagle facilitated the design process with its efficient and precise toolkit. This strategy combined compatibility, efficiency and flexibility in the board design, laying a solid foundation for control and monitoring systems.

4.2 Software

The software architecture of the microcontroller within this project was intentionally designed for modularity, allocating each component to its directory. This directory includes both `include` and `source` folders, ensuring a streamlined process for implementation. This structure significantly aids in integrating new components, as each function implementation is located in its distinct directory, encouraging a clean and organized structure easily scalable.

4.2.1 Current Measurement

For accurate current measurement, the selected ACS712 sensor and an Analog-to-Digital Converter (ADC) are utilised. The corresponding module is tasked with initializing the ADC and its ports, obtaining new measurements, and providing getter functions for accessing the data. Further analysis of the microcontroller architecture revealed that a single ADC, utilizing its built-in multiplexing capability represented as sequencers [33], is adequate for this task. This strategy efficiently minimizes resource usage on the board, enhancing overall system performance.

4.2.2 Solar Position and Motor Movement

The module for Solar Position and Motor Movement combines the precise calculation of the sun's position with the dynamic adjustment of the solar panel's orientation. The solar position calculation is essential for optimal panel orientation and utilizes a C-based code from the National Renewable Energy Laboratory [25]. Suitable for non-commercial

projects, this code aligns with the research and demonstration intentions. This algorithm, known for its accuracy, with an uncertainty of +/- 0.0003 degrees, calculates zenith and azimuth angles, requiring initialization with variables such as longitude, latitude, and time parameters. An update function allows for real-time adjustments to these initial values, adapting to changing environmental conditions.
Motor Movement complements this by adjusting the solar panel's angle to maximize energy capture, based on the solar position data. Key functions within this module include:

- The initialization function prepares the module for operation, setting up motor control parameters.
- A Snap Action Switch trigger function stops the motor responsible for the solar panel tilting angle, preventing overextension.
- The angle adjustment function aligns the solar panel with the calculated optimal solar position.
- The multiplexer control function directs the motor movement, ensuring precise positioning.

Together, these integrated modules support the project goals of modularity and efficient resource utilization, demonstrating a cohesive approach to solar panel orientation and energy management within the microcontroller software architecture.

5 Implementation

This chapter focuses on the implementation and setup of the circuit board designed for power management and motor control, as well as the diverse modules employed. It encloses both the hardware configuration of the devices and the software developed to meet the established requirements.

5.1 Hardware

This section details the development of the hardware for the weather station project's new board, enclosing the schematic design, board layout, and assembly process.

5.1.1 Pin Assigment

Prior to the schematic design, the assignment of the pins to each module is required. This process involved a meticulous analysis of each component's connection requirements, leading to their assignment for the appropriate signals. The table below presents the pin assignment, illustrating how each component is interfaced with the external signals:

Output Signals	**Component signals**
+12V	Voltage Converter IN
+5V	Voltage Converter SW_OUT
GND	Voltage Converter GND
PH0	Snap-Switch 1
PH1	Snap-Switch 2
GND	Snap-Switch GND
+12V	ACS712-MOTOR IP+
VDD_MOTOR	ACS712-MOTOR IP-
+5V	ACS712-MOTOR VCC
GND	ACS712-MOTOR GND
PE1	ACS712-MOTOR VIOUT
+5V	ACS712-TIVA IP+
VDD_TIVA_5V	ACS712-TIVA IP-
+5V	ACS712-TIVA VCC
GND	ACS712-TIVA GND
PE2	ACS712-TIVA VIOUT
SOLAR_IN	ACS712-SOLAR IP+
SOLAR_OUT	ACS712-SOLAR IP-
+5V	ACS712-SOLAR VCC
GND	ACS712-SOLAR GND
PD4	ACS712-SOLAR VIOUT
PF1	MUX 1Z
PF1	MUX 2Z
MOTOR1_PWM1	MUX 1Y0 & 1Y2
MOTOR1_PWM2	MUX 1Y1 & 1Y3
MOTOR2_PWM1	MUX 2Y0 & 2Y1
MOTOR2_PWM2	MUX 2Y2 & 2Y3
+5V	MUX VCC
GND	MUX GND
PN2	MUX S0
PN3	MUX S1
MOTOR1_PWM1	DRV8231-1 IN1
MOTOR1_PWM2	DRV8231-1 IN2
MOTOR_1+	DRV8231-1 OUT1
MOTOR_1-	DRV8231-1 OUT2
VDD_MOTOR	DRV8231-1 VM
+3.3V	DRV8231-1 VREF
GND	DRV8231-1 GND
MOTOR2_PWM1	DRV8231-2 IN1
MOTOR2_PWM2	DRV8231-2 IN2
MOTOR_2+	DRV8231-2 OUT1
MOTOR_2-	DRV8231-2 OUT2
VDD_MOTOR	DRV8231-2 VM
+3.3V	DRV8231-2 VREF
GND	DRV8231-2 GND

Table 5.1: Pin assignment for each component

Unused signals are left as open wires and in the schematic software are linked to a non-connected symbol, simplifying the design of the system and minimizing any potential errors.

5.1.2 Schematic Design

The process to design the schematic as explained in the concept plan, was done in Eagle. The strategy involved integrating the ports with their corresponding connections and incorporating every component symbol along with the essential parts.

The symbol and footprint for the chosen components were obtained as library packages from the Mouser Electronics shop [22], a supplier of authorized parts, ensuring precise dimensions and connection order for both the symbol and footprint.

The final result can be reviewed in the Appendix A

Ports

The ports are the only means to establish external connections as no wireless links are implemented for this board. To ensure stability during the solar alignment operations, the port connectors are to be secured to avoid possible disconnections. To satisfy the requirements, two types of connections were implemented from the industry standards: a screw terminal block for secure fixing of the wires and a female pin header for interfacing to the microcontroller board. The complete array of external connections is itemized in the following list, derived from the needs address in Table 5.1.

- JP3 & JP4: Connections to the previous board using the "2X4_STIFT_GEWINKELT" package, which is a standard right-angle female pin header.
- JP5: Connections to the previous board using the "2X4_STITF" package, which is a standard straight-pin connection.
- SNAP-SWITCH: Connections to the safety snap action switches, using the three positions pin header "MKDSN1,5/3-5,08" package.
- MOTOR_CON: Connection to both motors, using the "MKDSN1,5/4-5,08" package.

- EXT-CHARGER: Connections to an external charger such as a voltage generator, using the two positions pin header "MKDSN1,5/2-5,08" package.
- SUPPLY: Connections to the solar panel, accumulator and solar transformer, using the eight two positions pin header "MKDSN1,5/6-5,08" package.

Voltage Regulator

A switching voltage regulator by itself is of no use, as some complementary components are required for its operation. The essential piece for its function is an inductor capable of stabilizing the output supply to obtain a steady output, for when the voltage regulator cycle is low, the inductor would be partially discharged.

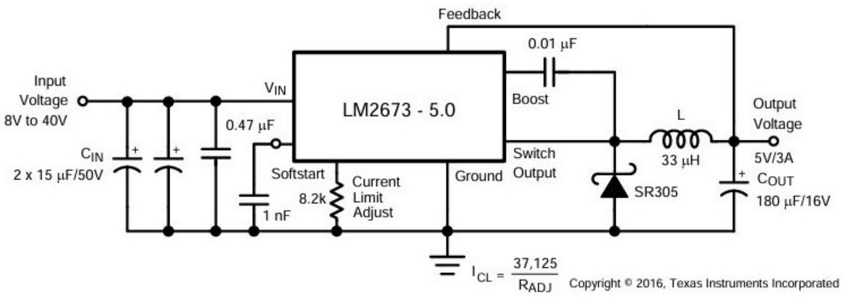

Figure 5.1: LM2673 Typical Aplication [35]

From examining the datasheet provided by the manufacturer [35], an intuitive schematic shown in Figure 5.1 is provided. Complementary to this, are some recommendations for the selection of specific component types and values. After proper analysis, the necessary components were implemented in the subsequent list.

- **Inductor**: The inductor selected was the Coilcraft MSS1210-473MED with a value of 47µH, chosen for its efficient energy storage and transfer capabilities during switch operations. Its compact ferrite drum core design significantly reduces electromagnetic interference (EMI), thus minimizing any compromise to the system's signal integrity. The selection follows the guidelines for maintaining a maximum ripple current at 30% of the load current, ensuring operational efficiency; this can be derived from a comprehensive table provided in the data sheet [35].

- **Adjustable Current Limit Resistor**: The value for RADJ must be carefully selected to precisely adjust the peak switch current of the LM2673. This choice was based on the need for a limiting current mechanism for the microcontroller, which has a limit of 1 A, in addition to the ACS712 current measurements and with the recommendation from the manufacturer of setting the peak switch current limit to be at least 50% greater than Iout maximum to allow for at least 30% inductor ripple current, a value of 1.65A is obtained. To properly calculate the resistor value, a simple equation from Figure 5.1 was solved.

$$R_{ADJ} = \frac{37,125}{1.65A} = 22500\,k\Omega$$

  As a resistor with value 22500 is not able in the standard size package 805, consequently a 22 kΩ was used.

- **Catch Diode**: The catch diode in the LM2673 circuit ensures continuous flow of current through the inductor during periods when the switch is deactivated. This is achieved by rerouting the current towards the ground, thus preventing any negative voltage drops beyond -1V. The Schottky diode SK32 was chosen based on the fact that it fulfils the requirements, including a Maximum Recurrent Peak Reverse Voltage of 20V, exceeding the safety requirement of 1.3 times the 12V input, and its low forward voltage drop, critical for maintaining high efficiency in the power supply circuit.

- **Input capacitor**: A 47 µF capacitor ensures that it can supply additional current and smooth out voltage variations during the dynamic load changes innate from high-current switching regulators. This choice is based on the provided table selection from the datasheet [35]. The capacitor is rated to manage half the peak of the DC load and to withstand voltage surges up to 1.3 times the highest input level. Additionally, its placement close to the LM2673's input pin minimizes inductance-related ringing, ensuring stable operation.

- **Output capacitor**: The selection of a 100 µF output capacitor helps smooth the DC output voltage and provides vital energy storage. This choice is informed by the provided table selection from the datasheet [35], underlining its low equivalent series resistance (ESR), a key factor affecting output ripple voltage and control loop stability. Adhering to datasheet guidelines, this specific capacitance and ESR contribute to the desired unity gain bandwidth, crucial for the circuit's operational stability.

- **Booster capacitor**: For all applications a 10 nF capacitor is recommended. This capacitor is in charge of creating a voltage used to overdrive the gate of the internal power MOSFET. This improves efficiency by minimizing the resistance of the switch and associated power loss.
- **Soft Startcapacitor**: A soft-start capacitor was not incorporated into the voltage regulator design, as it was determined to be non-essential for this application. The microcontroller's maximum current of 1A suggests that the inrush current will be manageable. This decision simplifies the design, focusing on components that are critical to achieving the project's objectives.

Current Measurement

The integration of ACS712 current measurement sensors was guided by the datasheet specifications [3], which outlined a typical application for interfacing with microcontroller ADCs within a 3.3V range. This was crucial for ensuring compatibility with the TIVA TM4C1292NCPDT microcontroller, characterized by its maximum ADC input voltage of 3.3 V [33]. To match the sensor output voltage with the microcontroller ADC input specifications, a voltage divider was utilized. This divider, composed of two resistors chosen following specifications from [3], effectively scaling down the sensor output to an appropriate 3.3 V level.

Moreover, to enhance signal quality, a 1 nF capacitor recommended by the datasheet was utilized to construct a filter with a defined bandwidth. Additionally, a filter resistor was also integrated into the output, establishing a low-pass filter. This configuration markedly improves the signal-to-noise ratio, thereby elevating the precision of the output signal.

Multiplexer

The connection to the multiplexer where done so that only one is required, as seen in the table below by carefully routing the motor 1 first connection to ports 1Y0 & 1Y2 and the second connection to 1Y1 & 1Y3, and the motor 2 first connectionas 2Y0 & 2Y1 and 2Y2 & 2Y3 to the second connection. All the scenarios are covered as seen in the table below.

S1	S0	Output	Motor 1	Motor 2
0	0	nY0	Forward	Forward
0	1	nY1	Forward	Backward
1	0	nY2	Backward	Forward
1	1	nY3	Backward	Backward

Table 5.2: Multiplexer modes

Furthermore, the connection to the Negative Voltage Supply (VEE) was tied to the ground, in response to the Tiva microcontroller low state being ground.

Motor Controller

For the module DRV8231, special attention was paid to the datasheet [34] recommendations, one of them being the addition of a 47 µF capacitor for voltage supply stabilization. Furthermore, to address the common issue of excess heat in motor controller modules, which can lead to overheating failures, the DRV8231 utilizes an innovative approach. Instead of traditional heatsinks on top of the package, it employs an external thermal resistor to effectively disperse heat, improving thermal management; additionally, the ground substrate is located under the package for heat transfer. The recommended 0.2 Ω thermal resistor can be split into five parallel resistors to manage high currents without excessive costs, as a unique resistor capable of doing that would be bulky and expensive.

$$R_{total} = \frac{R1 * R2 * R3 * R4 * R5}{R1 + R2 + R3 + R4 + R5} = \frac{1}{1+5} = 0.2\Omega$$

With this simple solution, the distribution of heat is more efficient and safer.

Snap Action Switches

For the detection of the switches, pull-up resistors were implemented, enabling the Tiva microcontroller to detect voltage rises upon switch activation.

The pull-up resistor where calculated using Ohm's law and the industry standard of 10 KΩ, reducing as much as possible the current consumption without compromising the stability of the pull-up resistor. The current through the resistor, when a switch is activated, is calculated as follows:

$$I = \frac{V}{R} = \frac{3.3\,V}{10\,k\Omega} = 0.33\,mA$$

Acumulator Charging

To ensure the safety of the solar panel, a protective Diode was placed between the solar panel and the external charging port of the accumulator. The SK32 Schottky diode [13], with its 20V Maximum Repetitive Reverse Voltage (VRRM) and 3A Maximum (average) Forward Furrent (IF(AV)), is specifically chosen for its ability to prevent reverse current flow into the solar panel. Exceeding more than the required 1.3 times the input voltage of 12 V and handling high currents, ensures the safeguard of the solar panel longevity and performance.

Light Emitting Diodes

LED indicators are utilized to display the status of various power supplies, with green LED colour being a common industry practice for representing correct operation. The specific packages that were employed were the ones available at the HAW, which are the standard 0805 size. As the LEDs are to be powered directly by the 12V and 5V power supply, a series resistor responsible for limiting the current that flows through the LED needs to be placed. The forward voltage for the green LED is 1.678V and a common forward current is approximately 20 mA, the values were obtained from [37], who used a multimeter to measure the forward voltage of the green LED. Nevertheless, to achieve a lower current consumption, the intensity of the light emitted by the LED can be reduced by lowering the desired current from 20 mA to 12 mA.
The required resistance for each LED can be calculated using Ohm's law:

$$R_{green12V} = \frac{12V - 1.678V}{12mA} \approx 860\Omega \qquad R_{green5V} = \frac{5V - 1.678V}{12mA} \approx 276\Omega$$

Given that these precise values are not readily achievable with standard resistor values, a compromise was made with the resistance values. For the 12V LED indicator, an 820 Ω resistor was selected, and for the 5V LED indicator, a 220 Ω resistor was used.

5.1.3 Board Design

The design of the printed circuit board (PCB) is a critical step in the development of the electronic system. This PCB utilizes a two-layer construction, which provides a balance between complexity and cost efficiency. The layers of a PCB refer to each thin sheet of conductive copper integrated into the circuit board, essential for routing electrical connections between components. Multilayer PCBs, constructed by laminating alternating layers of insulating and conductive materials, enable complex, dense circuitry within a compact footprint. They offer enhanced capacity and flexibility compared to single-layer boards but at a higher cost and complexity in fabrication and repair [27].

Figure 5.2: Two-layer PCB example extracted from [27]

The board design employs a two-layer construction, remarking an optimal balance between complexity and cost-effectiveness. The choice of a dual-layer structure is pivotal for enhanced heat dissipation, a critical aspect that will be elaborated on subsequently. For this specific project, opting for more than two layers would be unnecessary and could introduce unnecessary complexity. The two-layer approach allows for a better distribution of the connection and heat dissipation.

Connections between the top layer and the bottom layer are facilitated with through-hole vias. This type of via is the most commonly used in circuit boards. It consists of a hole drilled through the board using a mechanical drill, which is then plated with a conductive material. The size of the via varies depending on the signal requirements and the current it will carry.

During the PCB design process, guidelines established to ensure the integrity of the signal distribution and power supply are crucial to follow [5]. A key principle is a clear distinction between digital signals and power supplies to prevent interference, stressing the importance of routing digital traces away from power lines for the stable operation of digital components.

To optimize wire thickness for varying current demands, a worst-case scenario estimation was performed, resulting in the detailed current consumption analysis illustrated in the following table.

Component	Max current
Motor Controller (x2)	3.7 A
Multiplexer	0.16 mA
Voltage Regulator	6 mA
Current Sensor (x3)	0.01 A
Snap Action Switch (x2)	0.33 mA
Microcontroller PCB	1 A

Table 5.3: Current Consumption Worst Case Scenario.
The total maximum current consumption is approximately 8.44 A.

Considering a 1.2 Ampere hour (Ah) accumulator, as detailed in Table 4.3, and assuming all components operate at their maximum current without solar panel recharging, the setup would function for approximately 8.5 minutes, as depicted by the following formula.

$$\text{Battery Life (hours)} = \frac{\text{Battery Capacity (Ah)}}{\text{Current Draw (A)}} = \frac{1.2Ah}{8.44} \approx 8.5minutes$$

This current analysis leads to the conclusion that the maximum current for a power line could be 3.7 A, based on the motor controller rating. Regardless, actual current levels are expected to be lower due to reduced motor power through PWM control.

The PCB design incorporates wires of varying thicknesses to meet the specific current requirements of each component. The current carrying capacity of a trace is directly related to its width and thickness, with specifications for digital and power traces ensuring safe and efficient current conduction. Digital signal traces are designed with a width of 20 mil (milli-inches) and a clearance of 5 mil, capable of safely carrying up to 3 A at 60ºC, according to [8]. Power traces, designed to handle higher currents, are specified with a width of 50 mil and a clearance of 10 mil, allowing for a maximum current capacity of 6 A at the same temperature, thus preventing overheating or voltage drops that could impact system functionality.

The design of the printed circuit board (PCB) also integrates layout recommendations from the component datasheets, which provided specific guidelines on trace width, spacing, and other key parameters to ensure optimal functionality and reliability.

Further, the PCB layout features clearly labelled text for each component and connection, significantly facilitating assembly processes and demonstrations.

The final result can be reviewed in the Appendix A

Board Shape

The shape of the board was mirrored from the previous board, with a quarter of a circle design. This decision was made to maintain the aesthetics of the station, as it serves no practical purpose.

To maintain consistency in appearance, the solar charger (SOLAR-Laderegler 4A Typ 18123) component was positioned outside of the board on the aluminium frame of the solar panel. This decision was influenced by its lightweight and the improved visibility of its LED indicator.

Despite this, however, the accumulator needed space on the wood where the board is supported, as its weight and dimensions prevented placement on top of the PCB or the solar panel chassis. The battery location was chosen to minimize intrusion, near the center of the rotary table to maintain balance. This decision was informed by a demonstration conducted on the previous board.

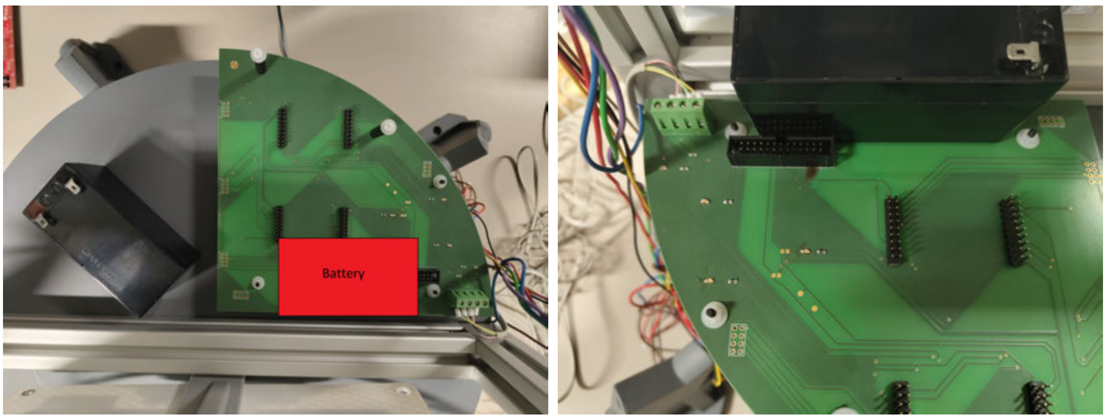

Figure 5.3: Testing of battery position on previous board

As it can be seen in Figure 5.3, the dimension of the battery aligned perfectly with the space. On the board design a space for the accumulator, with a width of 97 mm and a depth of 43 mm, was left with sufficient tolerance.

Component Layout

In designing the component layout, a deliberate effort was made to label the components based on their function, enhancing the board's readability and ease of understanding for a general audience. This strategic placement includes the voltage converters positioned at the top section of the board, the current measurement sensors located centrally, and additional voltage converters situated on the right. Such an organization not only aids in visual comprehension but also follows best practices as recommended in the components datasheets.

Furthermore, special attention was given to the layout of the switching voltage regulator. To mitigate the risk of electromagnetic interference (EMI) affecting other components, the regulator was placed at a considerable distance from other sensitive elements on the board. This precaution ensures that the regulator's switching operations do not compromise the performance and reliability of nearby components, adhering to guidelines for minimizing EMI in circuit design.

In addition, based on recommendations from the laboratory technician, holes for wires were added near the ports for the supply and motor. This modification aids in cable management, especially for the motor tasked with rotating the board.

Heat Management

Effective thermal management in PCB design is pivotal for preventing component overheating. It ensures that operations remain within safe temperature thresholds, thereby increasing reliability and prolonging the lifespan of the components. Key strategies for achieving efficient heat dissipation include the implementation of thermal vias and the utilization of ground planes [4]. Ground planes achieve two main objectives, acting as electrical return paths and thermal dissipation to evenly distribute heat across the board. Thermal vias complement this mechanism by promoting vertical heat transfer through the PCB layers, thereby enhancing the overall efficiency of the thermal management system.

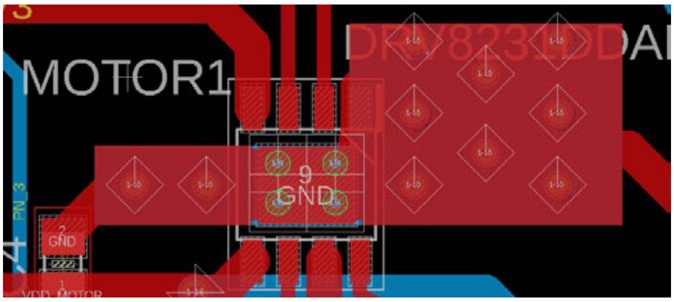

Figure 5.4: Illustration of the heat dissipation strategy in the design

As depicted in Figure 5.4, the above-mentioned techniques were implemented, incorporating ground planes and via connections for effective heat management. This integrated approach, emphasizing the use of a dual-layer strategy, plays a crucial role in enhancing the operational longevity of motor drivers particularly, especially when subjected to high current flow.

Routing

The routing process was meticulously planned to adhere to best practices in PCB design, emphasizing direct pathways while strategically separating digital and power signals to minimize interference. According to established guidelines [32], it is essential to focus on circuit performance, manufacturability, and component accessibility. Key to reducing electromagnetic interference (EMI) and signal reflection, the design avoids 90-degree angles in traces [21].

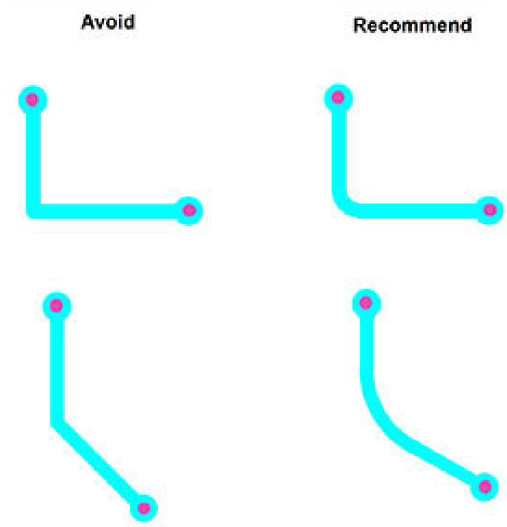

Figure 5.5: Hard corner example extracted from [28]

Challenges appeared with power signal widths, necessitating a 50 mil (milli-inches) width for high currents. This was problematic with smaller component pins, requiring another approach to prevent current spikes and EMI [21]. The solution involved using polygon shapes to form trapezoidal connections, adapting the base sizes to the wire widths, thus ensuring efficient routing and minimizing EMI risks.

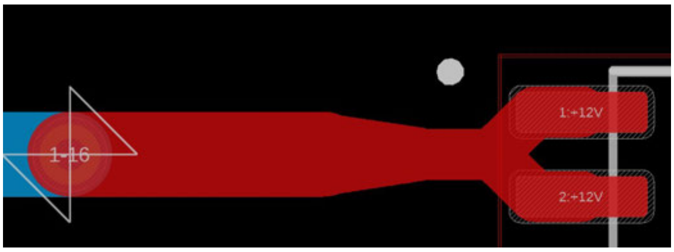

Figure 5.6: Teardrop impementation from own design

5.1.4 Board Assembly

The assembly of the board, with a long delay in its arrival, required swift action to solder all SMD components and necessary port headers. Utilizing soldering techniques [9], the process involved careful application of flux to ensure clean solder joints and prevent bridging or solder balls, which are common challenges with SMD components.

Detailed attention was given to each component's placement, ensuring alignment with the board's silkscreen indicators.

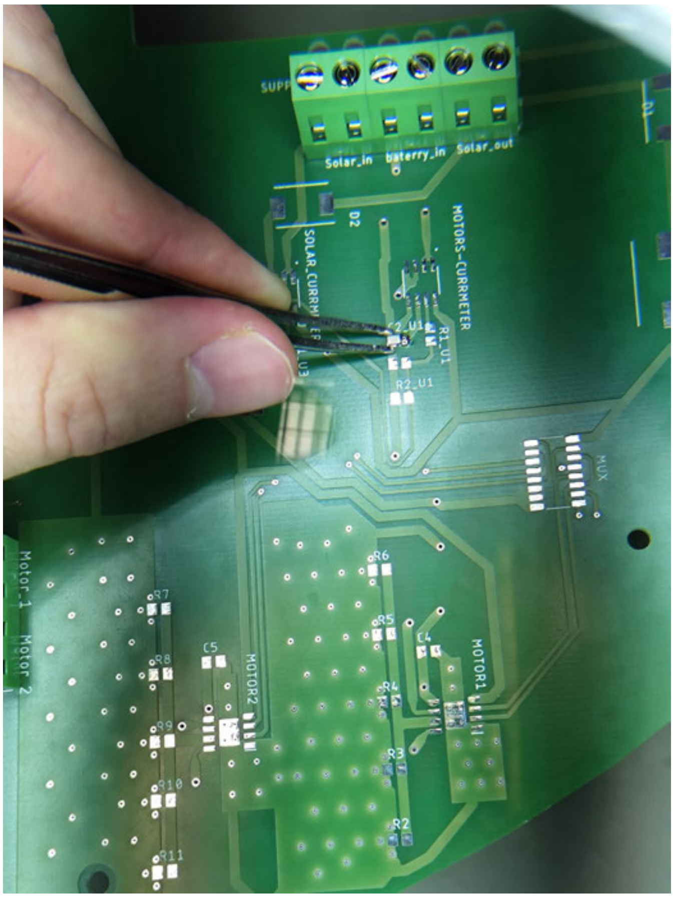

Figure 5.7: SMD soldering technique

Post-soldering, comprehensive visual inspection was practised on the board, supplemented by multimeter tests to check for shorts or open circuits. This step is crucial for identifying potential soldering defects before powering the board.

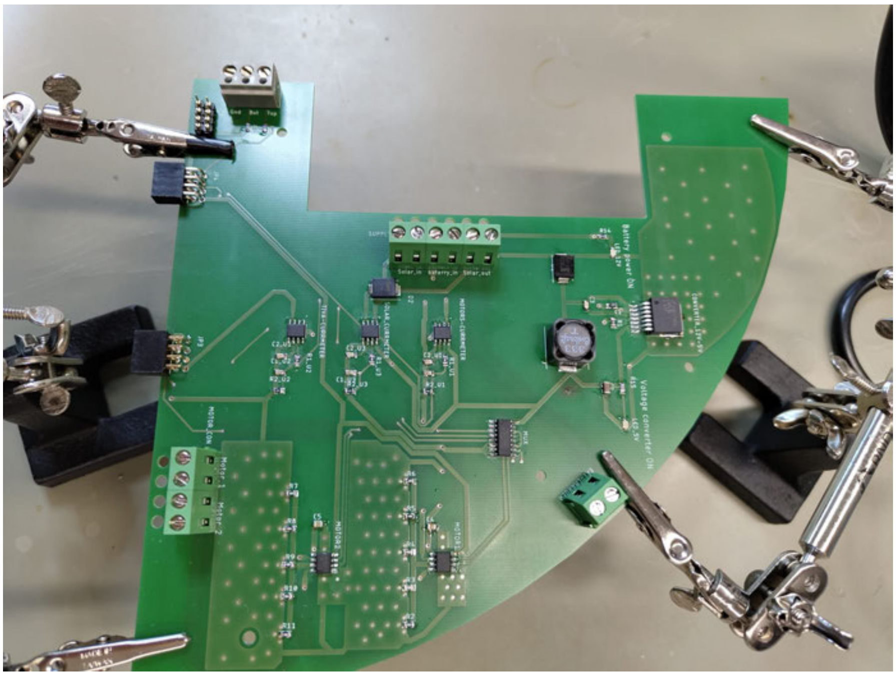

Figure 5.8: Populated board

Besides, the necessary jumpers on the microcontroller were adjusted to enable voltage supply from the booster pack, as detailed in [33].

5.1.5 Weather Station Assembly

The assembly of the weather station involved modifications to the station to accommodate the newly designed board. Precise holes were drilled into the existing structure to mount support stands, carefully aligning with the pre-existing board. Additionally, a dedicated hole was drilled for the cables of the motor responsible for base rotation, facilitating integration without compromising the station aesthetics.

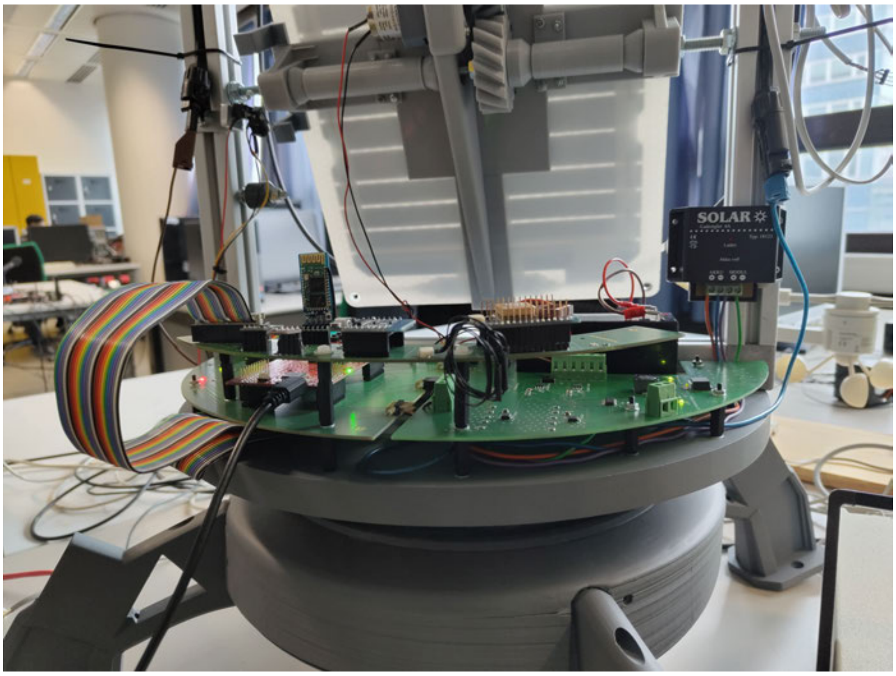

Figure 5.9: Finished Weather Station

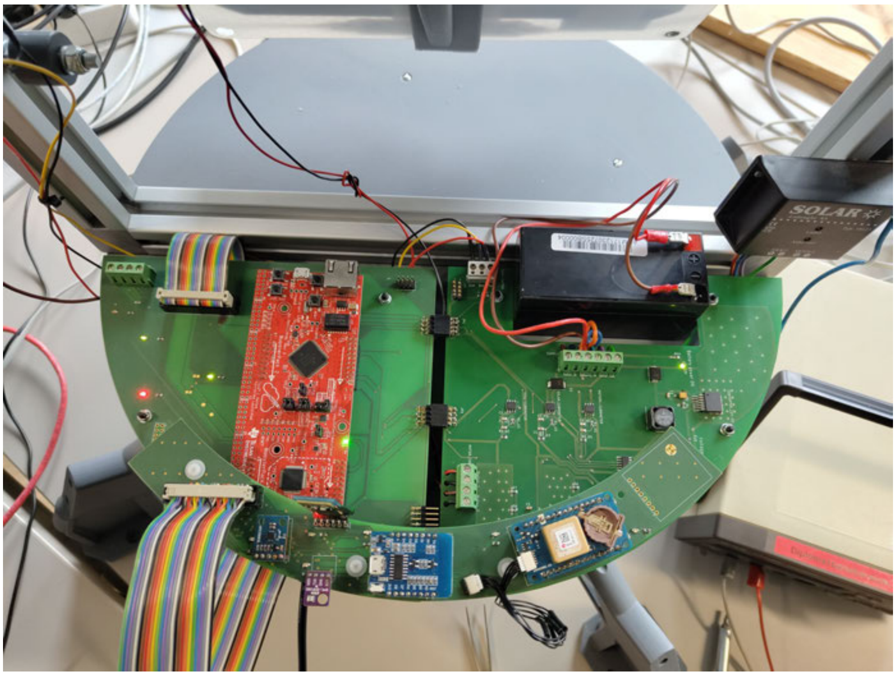

Figure 5.10: Finished Weather Station, zenithal view

The solar charger was securely mounted on the aluminium frame with screws, a decision made to facilitate the exhibition of its LEDs. The process of adapting cables was crucial, given the accumulator and each component's unique connectivity requirements. This approach was essential to secure and maintain reliable connections, thereby decreasing the risk of disconnections and potential safety hazards.

5.2 Software

This section explores the implementation of the software framework developed for the weather station project, emphasizing the architecture and functionalities embedded within it. The project software structure, as illustrated in Figure 5.11, showcases the hierarchical organization of the project files, encompassing documentation, implementation, and configuration settings essential for the operation of the weather station.

```
Weather Station
├── Documentation
│   ├── Datasheets
│   ├── Doxygen_Westermann
│   ├── PCB_Roldan-Rodriguez
│   └── PCB_Westermann
├── Implementation
│   ├── Components
│   │   ├── ACS712
│   │   ├── Anemometer
│   │   ├── bluetooth
│   │   ├── bme280
│   │   ├── driver_wrappers
│   │   ├── gps
│   │   ├── hmc5883l
│   │   ├── solar
│   │   ├── sys
│   │   └── wifi
│   ├── lib
│   │   └── TivaWare-2.1.4.178_short_cpy
│   ├── Startup
│   └── TargetConfiguration
└── targetConfigs
```

Figure 5.11: Project Directory Structure

The project file organization is pivotal for maintaining a structured and accessible codebase. As depicted in Figure 5.11, the project structure is divided into Documentation and Implementation sections.

- **Documentation**: This section houses critical resources such as Datasheets, Doxygen documentation for software code, and PCB designs. It provides an essential reference for future developers.
- **Implementation**: This section englobes the software development process, further subdivided into Components, Libraries, Startup routines, and TargetConfiguration. It contains low-level drivers, utility libraries, and initialization code necessary for the operation of the hardware components. Furthermore, each Component is organized into a source directory (`src`) and an include directory (`include`), supporting the project's modularity. This structure aids in distinguishing the functionalities of each component, promoting a clean and organized codebase.

5.2.1 Solar Position Algorithm

The integration of the Solar Position Algorithm (SPA) in the weather station solar panel system is key for optimizing energy capture. The SPA, based on NREL's model [24], calculates the sun's position by using geographical coordinates, annual average atmospheric readings, date, and time.

From the spa header file, the spa structure was used to initialize the required values. The annual average atmospherics could technically be obtained from the weather station itself, though it would require a year's worth of readings. Therefore default values were obtained from [39]. In addition, a wait function was implemented until the date, time, latitude and altitude values from the GPS module were obtained to avoid generating an error from the spa module.

While the system was designed to automatically adjust the solar panel orientation based on SPA outputs, including solar azimuth and zenith angles, the full automation through the Real Time Clock (RTC) module is still in progress, with only a foundational framework established. Currently, the system permits manual repositioning of the panel through Bluetooth commands, serving as a temporary solution pending the realization of full automation.

The intended automation involves operating an RTC interrupt, precisely the RTC match 0 used for hibernation protocols [37], to periodically trigger the panel alignment function, in addition to taking measurements, at a preferred interval of every 15 minutes. Additionally, auto-alignment is intended to activate only during daylight hours, which is already implemented in the "alignSP" function.

Bluetooth connectivity provides the flexibility for manual alignment adjustments and setting changes. It enriches user interaction and facilitates immediate panel orientation optimization. The system grants access to essential solar parameters such as azimuth and zenith angles, and sunrise and sunset times, via getter functions.

5.2.2 Motor Controller Functionality

This section outlines the motor control implementation for adjusting the solar panel's orientation. The method employs Pulse Width Modulation (PWM) for motor control, configured to a 50% duty cycle and an 80 kHz frequency using the system clock, implementing enough torque for the gears while reducing energy use and motor driver heat. The efficiency of this setup is illustrated in Figure 5.12, showing how the PWM's active duration impacts power delivery. Notably, only one PWM generator is used, with the microcontroller designed to independently toggle the two ports on or off, enhancing control flexibility and resource efficiency.

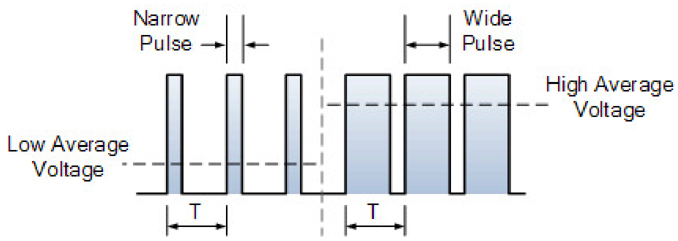

Figure 5.12: PWM signal representation extracted from [14]

As highlighted in Section 5.1.2, motor directional control is managed through a multiplexing strategy, necessitating GPIO initialization for the multiplexer signal handling. This allows for the individual directional adjustment of each motor. Appropriate direction implementation is enabled by locally storing each motor direction, adjustable via a setter function.

The system carefully tracks and internally stores the solar panel altitude and azimuth, offering getter functions for easy monitoring outside the module. Movement commands (start, stop, move to position) for each motor ensure full control over panel alignment. This modular design supports future integration, such as manual station control, by allowing these functions to be accessed across different system modules.

5.2.3 Interrupt Handler for Snap Action Switch

In the development of the interrupt handler for snap action switches, it was crucial to prioritize the handling of these interrupts carefully. Failure to promptly address these interrupts could result in an overload condition on the motor, risking significant damage to the solar panel or other components. To mitigate such risks, the interrupt priority levels have been carefully adjusted. Specifically, the priority for Bluetooth UART interrupt has been shifted from 0 (the highest level) to 1, acknowledging that while maintaining a Bluetooth connection is important, preventing physical damage to the system takes precedence. Furthermore, the implementation includes the initialization of a dedicated interrupt handler function. This function is tasked with stopping Motor 1, which is responsible for adjusting the tilt of the solar panel, thus safeguarding the hardware from potential harm. Additionally, a timer mechanism has been integrated to monitor and calculate the duration required for the solar panel to pivot from a 0º to 90º angle.

5.2.4 ACS712 Measurement Functionality

The ACS712 sensor integration is focused on accurately measuring the electrical current through various points on the weather station. This functionality allows the opportunity to identify and monitor the areas of greater energy consumption.

The output of the ACS712 is of the type Voltage, with a resolution step of 185 mV/A, indicating a 185 mV change per ampere. An ADC from the Tiva microcontroller, specifically only the ADC 0 with multiplexing functionality, is operated to convert this analogue signal to digital, optimizing resource use. The multiplexing process involves sampling each sensor and storing the data in a FIFO (First In First Out) buffer [12], A FIFO buffer operates much like a queue, processing the first entered data first, as depicted in a referenced in Figure 5.13. This structure ensures data is handled in the order it arrives.

Once a value is read from the FIFO, it is removed, and the system moves to the next entry, maintaining an orderly flow of data processing.

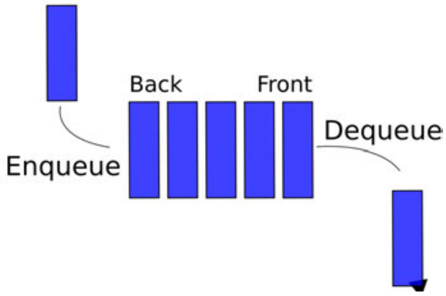

Figure 5.13: FIFO representation extracted from [20]

The C file includes initializing the ADC 0, capturing new samples, converting these to current values, and providing access through getter functions. A dedicated function converts ADC values to current by translating voltage readings into current, factoring in the ACS712 sensitivity and voltage offset at zero current, with the offset determined by the sensor's voltage supply and the voltage divider [3].

5.2.5 Previous Software Integration

Integrating with the existing software required a structural transition from individual developer directories to a unified component-focused strategy. This reorganization not only promoted greater collaboration but also simplified the development process, leading to a more user-friendly environment. For example, connectivity modules were moved from the previous folder `"Hasanova_BA"` to the `"Components"` folder. Additional adjustments were implemented to interact with the modules developed.

Adjustments to the `main.c` file included:

- Developing string-getter functions for enhanced system monitoring, current measurements, power statistics, and solar panel orientation to facilitate comprehensive system analysis.
- Enabling the solar tracking system to operate automatically, optimizing solar energy capture without manual intervention.

- Streamlining initialization routines for the ACS712 sensor, solar panel, and motor controls.

Modifications to Bluetooth command functionalities involved:

- Adding commands to toggle auto-alignment, offering users direct manipulation over the solar panel's orientation for maximum energy efficiency.
- Upgrading the system's capability to fetch detailed power statistics and tracking information, thereby enhancing user engagement and providing valuable insights into the system's performance.

Command	Description
AT+CALIGN!	Request alignment of the solar panel
AT+CPWR?	Check current measurements
AT+CTRACK?	Get if the solar panel is being tracked or not
AT+CTRACK	Set on/off the solar panel tracking

Table 5.4: Modified Bluetooth AT Commands

The adjustments, especially the improved accessibility of Bluetooth commands, seen in Table 5.4, and the implementation of new module setups, have been crucial for improving system usability. These changes, inspired by the user interaction structure outlined by [17], underlines a deep commitment to maintaining the system functionality while significantly improving user engagement and overall experience.

6 Results and Evaluation

This chapter evaluates the performance of the system post-implementation, comparing the testing outcomes with the requirements outlined in Section 3. It focuses on estimating how well the implemented functionalities align with the predefined objectives, identifying key achievements and areas for improvement.

6.1 Test Results

The evaluation of test results is divided into two distinct phases: pre-board assembly and post-board assembly. This bifurcation ensures comprehensive testing of each component individually before integration, as well as the assessment of the fully assembled PCB functionality.

6.1.1 Pre-Board Assembly

Motor Driver

The motor driver component was evaluated using the microcontroller PWM (Pulse Width Modulation) output. The initial test configuration consisted of a 1 kHz frequency and a 10% duty cycle, as illustrated in Figure 6.1.

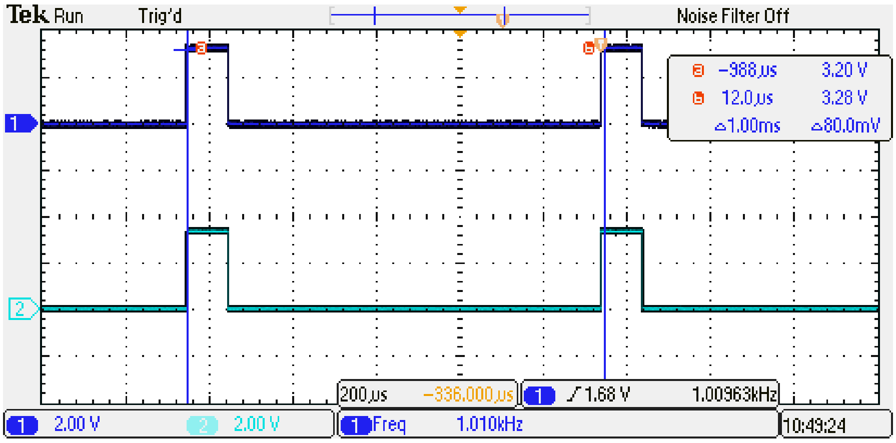

Figure 6.1: Microcontroller PWM output

The frequency of the signal is evident in its period, with 1000 Hz (s^{-1}) correlating to a 1 ms period. The logic high state voltage of the TIVA microcontroller is 3.3V [33], indicating the signal peak voltage is consistent with an oscilloscope reading of 3.3V.

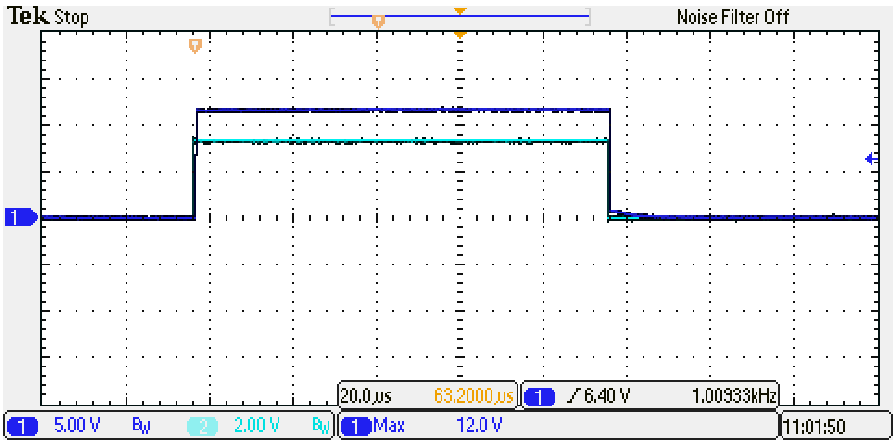

Figure 6.2: Output of DRV8231 motor driver

A test circuit was assembled in alignment with the board schematic, the output can be seen in Figure 6.2. As expected from [34], the output displays minor delays due to switching delays and the capacitive load inherent in the device. Following this, the motor controller was connected to the motor for further testing. Through a series of iterations, it was established that the motor load optimal operational parameters were a frequency of 80 kHz and a duty cycle of 50%. This adjustment notably improved the motor torque, facilitating the efficient driving of gears responsible for the solar panel.

Snap Action Switch

Testing the microcontroller interrupt functionality with snap action switches was essential to ensure the safety mechanism for preventing potential damage due to motor or solar panel overstrain. This test involved connecting the switches, each equipped with its respective pull-up resistor, to the designated port on the microcontroller. Manually activating the switches triggered an interrupt, stopping motor operations.

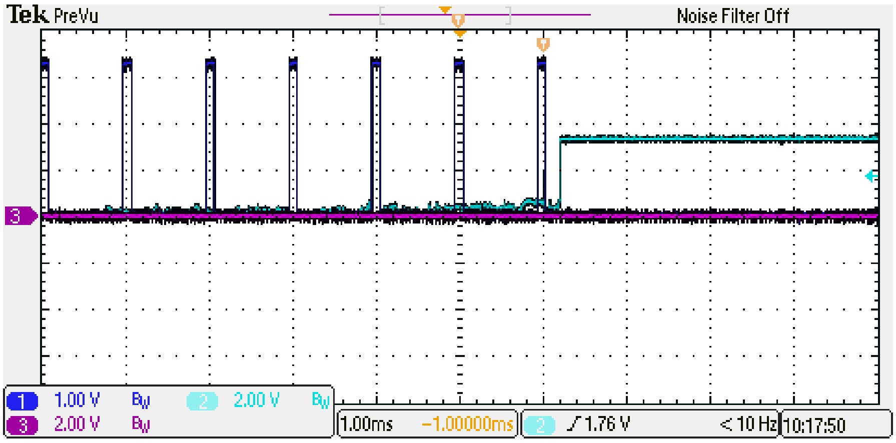

Figure 6.3: Testing of the Snap Action Switch Interrupts

Figure 6.3 illustrates the test result, where the PWM signal (shown in blue) is interrupted upon the activation of the snap action switch (represented by the cyan signal). This confirms the effectiveness of the switch integration and functionality in the system safety design.

Solar Position Algorithm

The Solar Position Algorithm (SPA) underwent testing to validate its predicting solar position capacities. Utilizing data from SunCalc as a benchmark [30], a comparative analysis was conducted. The results indicated that the SPA's calculations closely align with the benchmark, manifesting a deviation of merely 2%. This level of accuracy confirms the SPA's efficacy for reliable solar tracking in the system.

Calibration of Compass

The integration of the compass into the sensor board highlighted an alignment discrepancy with the orientation of the solar panel, necessitating angular calibration. Utilizing a digital compass with moderate precision, the procedure aimed to quantify this misalignment. Results revealed a 95º discrepancy between the solar panel direction and the HMC5883L compass readings. Notably, the reliability of the compass was compromised indoors due to its sensitivity to electromagnetic disturbances, underscoring the influence of environmental factors on its performance.

Current Measurement

For the ACS712 component testing, the design circuit combined with a simple addition was assembled. The addition involved connecting a 1 Ω resistor to generate a current flow, with the output voltage from the device measured by a multimeter for precision. This output voltage is crucial, as it is intended to be input into the microcontroller ADC.

Input Current	**Output Voltage**
0 A	2.125 V
0.502 A	2.218 V
0.706 A	2.254 V
1.05 A	2.317 V
1.496 A	2.402 V

Table 6.1: ACS712 testing results.

Additionally, a function generator was used as a voltage source to create a variable current, however, the function generator produced a limited maximum current of only 0.04 A. This limitation became evident in the output voltage from the ACS712, as illustrated in Figure 6.4, which did not achieve the anticipated precision due to the subtle variation in current. This observation underscores the importance of the ACS712 sensor's specified accuracy of approximately 0.185 V per Ampere [3].

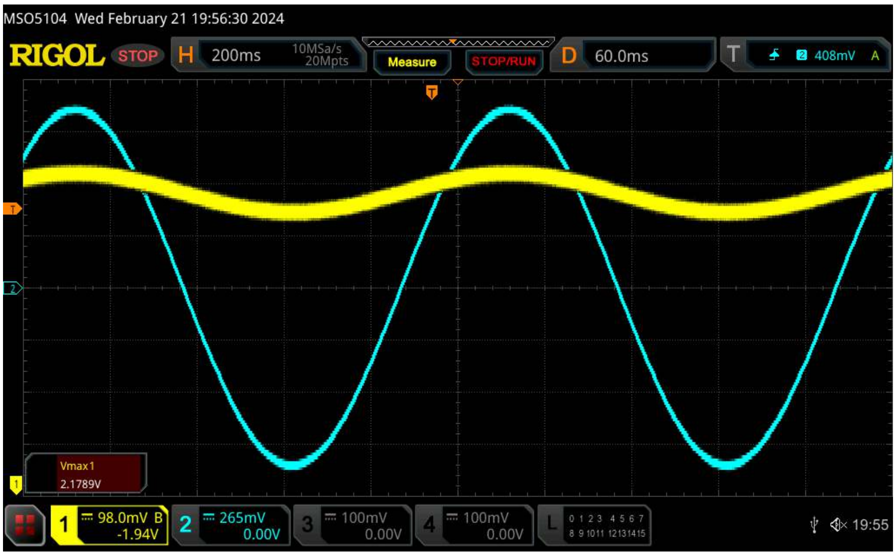

Figure 6.4: Sine input test for the ACS712.

Moreover, the microcontroller ADC (Analog-to-Digital Converter) ports were evaluated within a range of voltages to ensure correct functioning. This verification process was aimed at securing reliable operation and minimizing the need for debugging in a fully integrated system.

6.1.2 Post-Board Assembly

Following the assembly of the weather station, a series of focused tests were conducted to ensure the system functionality aligned with predefined requirements. Given the limited time, only an afternoon after assembly due to the delayed arrival of the board, the tests were strategically prioritized to verify the supply board core performance.

Autonomous Supply

To accurately evaluate the autonomy of the weather station and power efficiency, a series of tests were conducted. These tests aimed to simulate normal operational activities, including the activation of motors, retrieval of data samples from the sensor board, and establishing connectivity. This evaluation confirmed the system's capability to function autonomously, without the necessity for an external voltage source.

In addition, an effort was made to test solar charging, but the lack of sufficient sunlight made it challenging to conclusively determine whether the accumulator was being charged effectively.

Solar Alignment and Movement

An initial test was attempted, but the gears responsible for the tilt of the solar panel were found to be worn out. This problem prevents the solar panel from adjusting its position in response to motor rotation. Nevertheless, the other motor responsible for the base rotation was functioning as intended. Further repairs and investigations will be conducted after the submission to ensure an operational weather station.

6.2 Evaluation

This section evaluates the tests conducted against the project's hardware and software requirements. These tests covered essential functionalities including power management, solar panel operation, software efficiency, and user interface design, demonstrating compliance with both functional (F) and non-functional (NF) requirements. However, external factors prevented a careful post-assembly analysis of the station. Specific requirements, including station orientation and current measurement, were unverified due to time limitations. Furthermore, requirement 17, which involves periodic current readings for system restarts, remains partially addressed due to integration challenges, for the previous functionality related to the hibernation and RTC provided by [37] was nonoperational. Future work will aim to complete this integration, enhancing the automation system.

Although documentation efforts were defined, including detailed descriptions in this document and code comments, a complete guide could not be developed within the project timeline. This aspect underscores the need for further documentation work to ensure user-friendly operation and maintenance of the system.

Overall, the testing phase, specifically the pre-assembly phase, confirmed that the weather station and specifically the power supply board could fulfil the set requirements. However, it is not yet ready for demonstrations.

7 Conclusion

7.1 Summary

The journey of designing and implementing an autonomous weather station equipped with an optimized power supply system and a motor control board for a solar panel culminated in a project that addressed the technical challenges. The integration of a microprocessor-controlled power supply, alongside dynamic adjustments for solar panels, demonstrated a unified combination of hardware and software solutions.

The project, while ambitious in its scope, encountered real-world challenges such as tight schedules and unexpected delays in the delivery of the PCB. These obstacles, however, served as valuable learning experiences, improving the ability to manage stress and adapt to unforeseen circumstances, ultimately reinforcing the importance of resilience and flexibility in project management.

Consequently, this project presented the comprehensive knowledge and experience gained by students from both computer science and electrical engineering disciplines at the Hamburg University of Applied Sciences. It stands as a testament to the practical application of academic knowledge, encouraging a deeper understanding of the complexities involved in developing sustainable technologies. The project significantly contributed to academic development, providing a solid foundation for future efforts in the field of technology and sustainability.

In conclusion, the autonomous weather station project, although not fully archiving all the initial goals, provides a beneficial learning platform, preparing for the challenges and opportunities that lie ahead in professional careers. It highlighted the importance of interdisciplinary collaboration, adaptability, and continuous learning, principles that are essential for success in the rapidly evolving field of technology.

7.2 Future Outlook

The future improvements for the project are both ambitious and important for its development. The integration of an SD card, a preliminary task initiated by previous work [37], represents a significant upgrade for the system data logging capabilities. This modification is expected to enable offline data analysis and support backup functionalities.

Reexamining the server architecture is another crucial step. The aim is to transition from an opaque, 'black box' model to a system characterized by transparency, efficiency, and maintainability, thus rectifying current shortcomings.

The development of a dedicated mobile application stands out as a promising way to increase user engagement. This application would facilitate interactive remote station management, including configuration adjustments, data visualization, and controlling the alignment of the solar panel through Bluetooth connectivity.

Moreover, the implementation of energy-saving strategies with the help of timers and hibernation mode, will greatly contribute to power conservation. A foundational framework for these measures has already been established, though it is not yet functional. Once operational, these strategies are designed to allow the station to periodically switch to a low-power state, waking only for essential operations such as data sampling and solar panel realignment.

Lastly, enhancing the station data management protocols by developing regular data collection routines and automating the upload process to both the server and the SD card is essential. Adopting this approach will ensure data redundancy and accessibility.

Bibliography

[1] Conrad Electronic SE (Veranst.): *Conrad Electronic*. https://www.conrad.de/. – Accessed on: Feb. 22, 2024

[2] Mouser Electronics (Veranst.): *Mouser Electronics*. https://www.mouser.com/. – Accessed on: Feb. 22, 2024

[3] Allegro MicroSystems: *ACS712 Fully Integrated, Hall-Effect-Based Linear Current Sensor IC with 2.1 kVRMS Voltage Isolation and a Low-Resistance Current Conductor*. Manchester, New Hampshire, USA: Allegro MicroSystems (Veranst.), 2023. – Accessed on: Feb. 17, 2024

[4] Altium: *Circuit Board Thermal Analysis*. https://resources.altium.com/p/circuit-board-thermal-analysis. 2024. – Accessed on: Feb. 24, 2024

[5] Altium: *PCB Layout Guidelines*. https://resources.altium.com/p/pcb-layout-guidelines. 2024. – Accessed on: Feb. 24, 2024

[6] Arduino: *Arduino Official Website*. https://www.arduino.cc/. 2024. – Accessed on: Feb. 24, 2024

[7] Autodesk: *Autodesk EAGLE Overview*. https://www.autodesk.com/products/eagle/overview?term=1-YEAR&tab=subscription. 2024. – Accessed on: Jan. 5, 2024

[8] Beta LAYOUT GmbH: *PCB Spezifikationen*. https://de.beta-layout.com/leiterplatten/infos/spezifikationen/#1. 2022. – Accessed on: July 22, 2022

[9] Build Electronic Circuits: *SMD Soldering Guide*. https://www.build-electronic-circuits.com/smd-soldering/. 2024. – Accessed on: Feb. 24, 2024

[10] BYJU'S: *DC Motor*. https://byjus.com/physics/dc-motor/. 2024. – Accessed on: Feb. 24, 2024

[11] Cadence Design Systems: *Using a Switching Regulator vs. Linear Regulator for DC-DC Conversion.* Cadence PCB Design & Analysis Blog. 2020. – URL https://resources.pcb.cadence.com/blog/2020-using-a-switching-regulator-vs-linear-regulator-for-dc-dc-conversion. – Accessed on: Feb. 24, 2024

[12] Cummings, Clifford: *Synthesis and Scripting Techniques for Designing Multi-Asynchronous Clock Designs.* http://www.sunburst-design.com/papers/CummingsSNUG2002SJ_FIFO2.pdf. 2002. – Accessed on: Feb. 24, 2024

[13] Diodes Incorporated: *DS13006 High-Current/Voltage Darlington Arrays.* Plano, Texas, USA: Diodes Incorporated (Veranst.), 2020. – Accessed: [Insert Access Date Here]

[14] Electronics Tutorials: *PWM (Pulse Width Modulation) Illustration.* https://www.electronics-tutorials.ws/wp-content/uploads/2018/05/articles-pwm2.gif. 2018. – Accessed on: Feb. 24, 2024

[15] Electronics Tutorials: *Hall Effect - Explanation and Application.* https://www.electronics-tutorials.ws/electromagnetism/hall-effect.html. 2024. – Accessed on: Feb. 24, 2024

[16] Gaonkar, Ramesh S.: *Fundamentals of Microcontrollers and Applications in Embedded Systems with PIC Microcontrollers.* 1st. Boston, Massachusetts, USA : Thomson/Delmar Learning, 2006

[17] Hasanova, A. A.: *Design and development of wireless communication systems for control and monitoring of an autonomous meteorological station.* Hamburg. 2021

[18] How2Electronics: *Switched Mode Power Supply: SMPS Design & Applications.* https://how2electronics.com/switched-mode-power-supply-smps-design-applications/. 2023. – Accessed: Mar. 5, 2024

[19] Idzkiewicz, Przemyslaw ".: *Illumination of Earth by the Sun on the day of the winter solstice in the northern hemisphere.* NASA. – URL https://upload.wikimedia.org/wikipedia/commons/4/4d/Earth-lighting-winter-solstice_EN.png. – Composite image using "Earth's City Lights", "The Blue Marble: Land Surface, Ocean Color and Sea Ice" by NASA and illumination maps by John Walker's "Home Planet". Available under cc-by-sa license. Accessed: 29.01.2024

[20] Inductiveload: *Data Queue*. https://commons.wikimedia.org/wiki/File:Data_Queue.svg. 2008. – Accessed on: Feb. 24, 2024

[21] Montrose, M.I.: Time and frequency domain analysis for right angle corners on printed circuit board traces. In: *1998 IEEE EMC Symposium. International Symposium on Electromagnetic Compatibility. Symposium Record (Cat. No.98CH36253)* Bd. 1, 1998, S. 551–556 vol.1

[22] Mouser Electronics: *Downloadable Libraries for Schematics and Board Design*. 2024. – URL https://www.mouser.com/. – Accessed on: Feb. 17, 2024. Libraries for various electronic components and modules.

[23] Mouser Electronics: *TI EK-TM4C1294XL Board Callouts Image*. https://www.mouser.de/images/marketingid/2014/microsites/120178108/TI_EK-TM4C1294XL_board-callouts.png. 2024. – Accessed on: Feb. 24, 2024

[24] National Renewable Energy Laboratory: *Solar Position Algorithm for Solar Radiation Applications (Revised)*. 2008. – Supercedes November 2005 version

[25] National Renewable Energy Laboratory: *Solar Position Algorithm (SPA) Code*. 2023. – URL https://midcdmz.nrel.gov/spa/. – Accessed on: Feb. 14, 2024. Code available for solar position calculations.

[26] Palmetto Learning Center: *Are Sun-Tracking Solar Panels Worth It?* https://palmetto.com/learning-center/blog/sun-tracking-solar-panels-worth-it. 2023. – Accessed on: Feb. 24, 2024

[27] PCBASIC: *Understanding PCB Layers: What You Need to Know*. https://www.pcbasic.com/blog/pcb-layers.html. 2024. – Accessed on: Feb. 24, 2024

[28] Qualieco Circuits: *Design Tips for PCB Manufacturing - Figure 1*. https://www.qualiecocircuits.com.au/img/design-tips-pcb-manufacturing-figure-1.jpg. 2023. – Accessed on: Feb. 24, 2024

[29] Stuff, Engineering: *What Is DC Motor*. https://engineeringstuff.co.in/what-is-dc-motor/. 2024. – Accessed on: Feb. 24, 2024

[30] SunCalc: *SunCalc - Sun Position, Sunrise, and Sunset Calculator*. https://www.suncalc.org. 2024. – Accessed on: Feb. 24, 2024

[31] Symmetry Electronics: *MAG26-2791 Image*. https://www.symmetryelectronics.com/getmedia/c1e92ff4-8039-4501-b3a2-e0645e4f2815/mag26-2791.gif. 2024. – Accessed on: Feb. 24, 2024

[32] Systems, Cadence D.: *PCB Design Layout Guidelines for Engineers*. https://resources.pcb.cadence.com/blog/2023-pcb-design-layout-guidelines-for-engineers. 2023. – Accessed on: Feb. 24, 2024

[33] Texas Instruments: *Tiva™ TM4C1294NCPDT Microcontroller Data Sheet*. Dallas, Texas, USA: Texas Instruments (Veranst.), 2014. – DS-TM4C1294NCPDT-15863.2743, SPMS433B

[34] Texas Instruments: *DRV8231 Motor Driver Datasheet*. Dallas, Texas, USA: Texas Instruments (Veranst.), 2023. – SLVSA73E –SEPTEMBER 2013–REVISED MAY 2023

[35] Texas Instruments: *LM2673 SIMPLE SWITCHER® 3-A Step-Down Voltage Regulator With Adjustable Current Limit Datasheet*. Dallas, Texas, USA: Texas Instruments (Veranst.), 2023. – SLVS312D –NOVEMBER 1999–REVISED APRIL 2023

[36] Valvano, Jonathan W.: *Embedded Systems: Real-Time Interfacing to Arm® Cortex™-M Microcontrollers*. 2nd. USA : CreateSpace Independent Publishing Platform, 2012. – ISBN 978-1463590154

[37] Westermann, P. D.: *Design and Implementation of Hardware and Software for a Microcontroller-Controlled Sensor Module in a Weather Station*. Hamburg. 2022

[38] Wikipedia: *Azimuth and Altitude Schematic*. https://upload.wikimedia.org/wikipedia/commons/f/f7/Azimuth-Altitude_schematic.svg. n.d.. – Accessed: 29.01.2024

[39] World Weather Online: *Hamburg Weather Averages*. https://www.worldweatheronline.com/hamburg-weather-averages/hamburg/de.aspx. 2024. – Accessed on: Feb. 24, 2024

A Appendix - Board Design

All schematics fromt the board are in DIN-A4 size. These cover a page each and are laid out in the following pages in this order:

1. Board layout
2. Schematic connections
3. Schematic current measurement modules
4. Schematic voltage regulator 12V-5V
5. Schematic motors controller

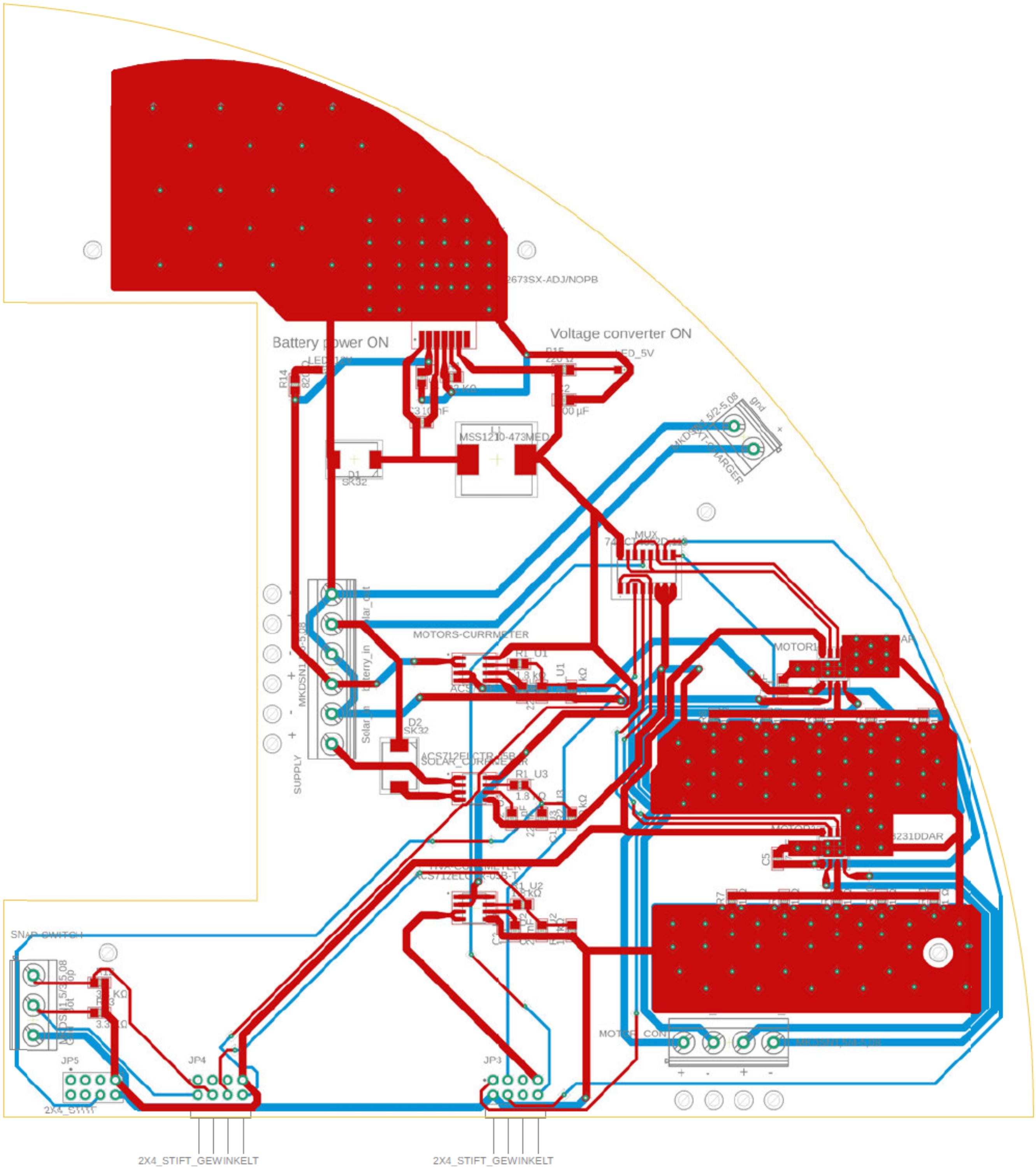
Battery power ON
Voltage converter ON
R14
R15
LED_5V
MSS1210-473MED
D1
SK32
D2
SK32
MUX
MOTORS-CURRMETER
R1_U1
U1
SOLAR_CURRMETER
R1_U3
U3
U2
SUPPLY
MOTOR1
C5
SNAP-SWITCH
JP5
JP4
JP3
2X4_STIFT_GEWINKELT
2X4_STIFT_GEWINKELT

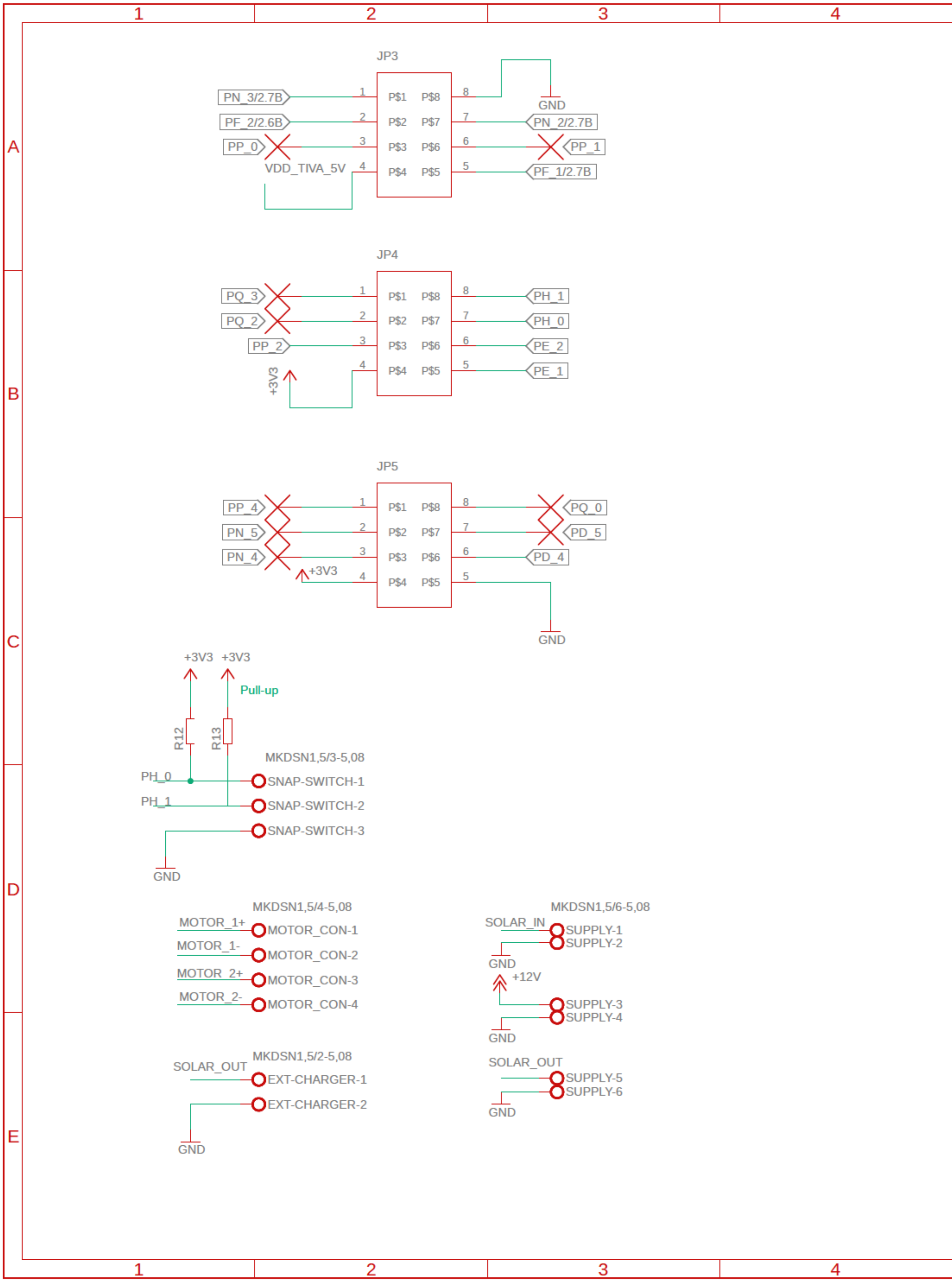
JP3
PN_3/2.7B
PF_2/2.6B
PP_0
VDD_TIVA_5V
GND
PN_2/2.7B
PP_1
PF_1/2.7B
P$1 P$8
P$2 P$7
P$3 P$6
P$4 P$5
JP4
PQ_3
PQ_2
PP_2
+3V3
PH_1
PH_0
PE_2
PE_1
JP5
PP_4
PN_5
PN_4
+3V3
PQ_0
PD_5
PD_4
GND
+3V3 +3V3
Pull-up
R12
R13
MKDSN1,5/3-5,08
PH_0
PH_1
SNAP-SWITCH-1
SNAP-SWITCH-2
SNAP-SWITCH-3
GND
MKDSN1,5/4-5,08
MOTOR_1+
MOTOR_1-
MOTOR_2+
MOTOR_2-
MOTOR_CON-1
MOTOR_CON-2
MOTOR_CON-3
MOTOR_CON-4
MKDSN1,5/2-5,08
SOLAR_OUT
EXT-CHARGER-1
EXT-CHARGER-2
GND
MKDSN1,5/6-5,08
SOLAR_IN
SUPPLY-1
SUPPLY-2
GND
+12V
SUPPLY-3
SUPPLY-4
GND
SOLAR_OUT
SUPPLY-5
SUPPLY-6
GND

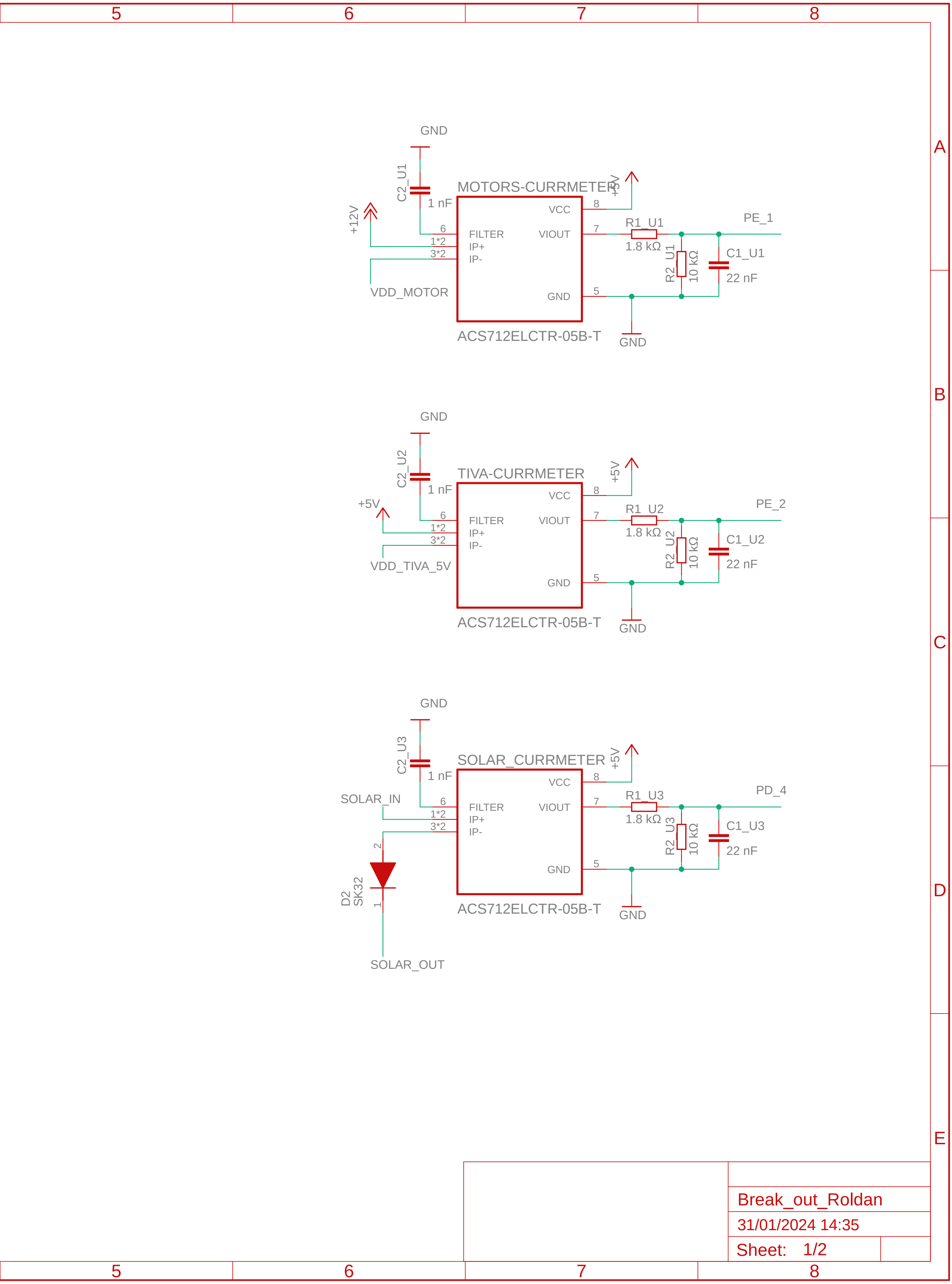

5
6
7
8
A
B
C
D
E
GND
C2_U1
1 nF
MOTORS-CURRMETER
+5V
+12V
VCC
FILTER
VIOUT
IP+
IP-
GND
R1_U1
1.8 kΩ
PE_1
R2_U1
10 kΩ
C1_U1
22 nF
VDD_MOTOR
ACS712ELCTR-05B-T
GND
GND
C2_U2
1 nF
TIVA-CURRMETER
+5V
+5V
R1_U2
1.8 kΩ
PE_2
R2_U2
10 kΩ
C1_U2
22 nF
VDD_TIVA_5V
ACS712ELCTR-05B-T
GND
GND
C2_U3
1 nF
SOLAR_CURRMETER
+5V
SOLAR_IN
R1_U3
1.8 kΩ
PD_4
R2_U3
10 kΩ
C1_U3
22 nF
D2
SK32
ACS712ELCTR-05B-T
GND
SOLAR_OUT
Break_out_Roldan
31/01/2024 14:35
Sheet: 1/2

	1	2	3	4

A

B

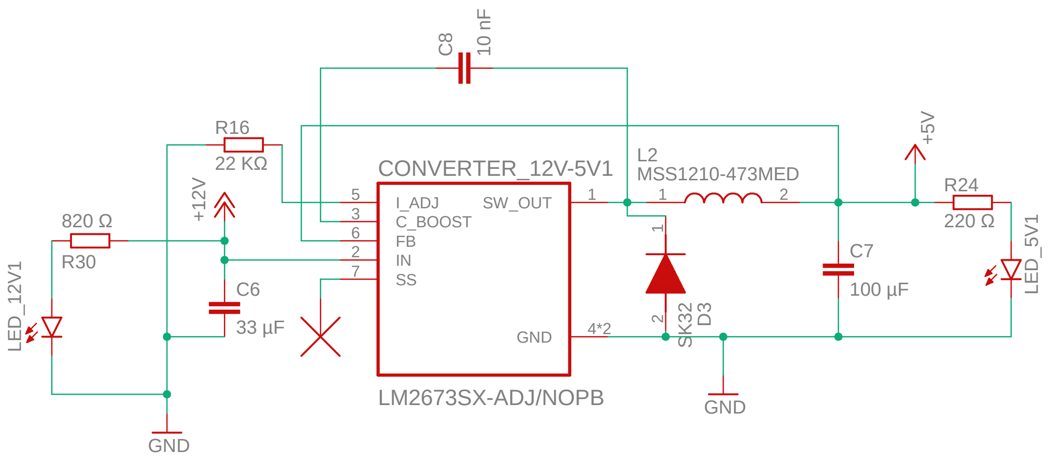

C

D

E

	1	2	3	4

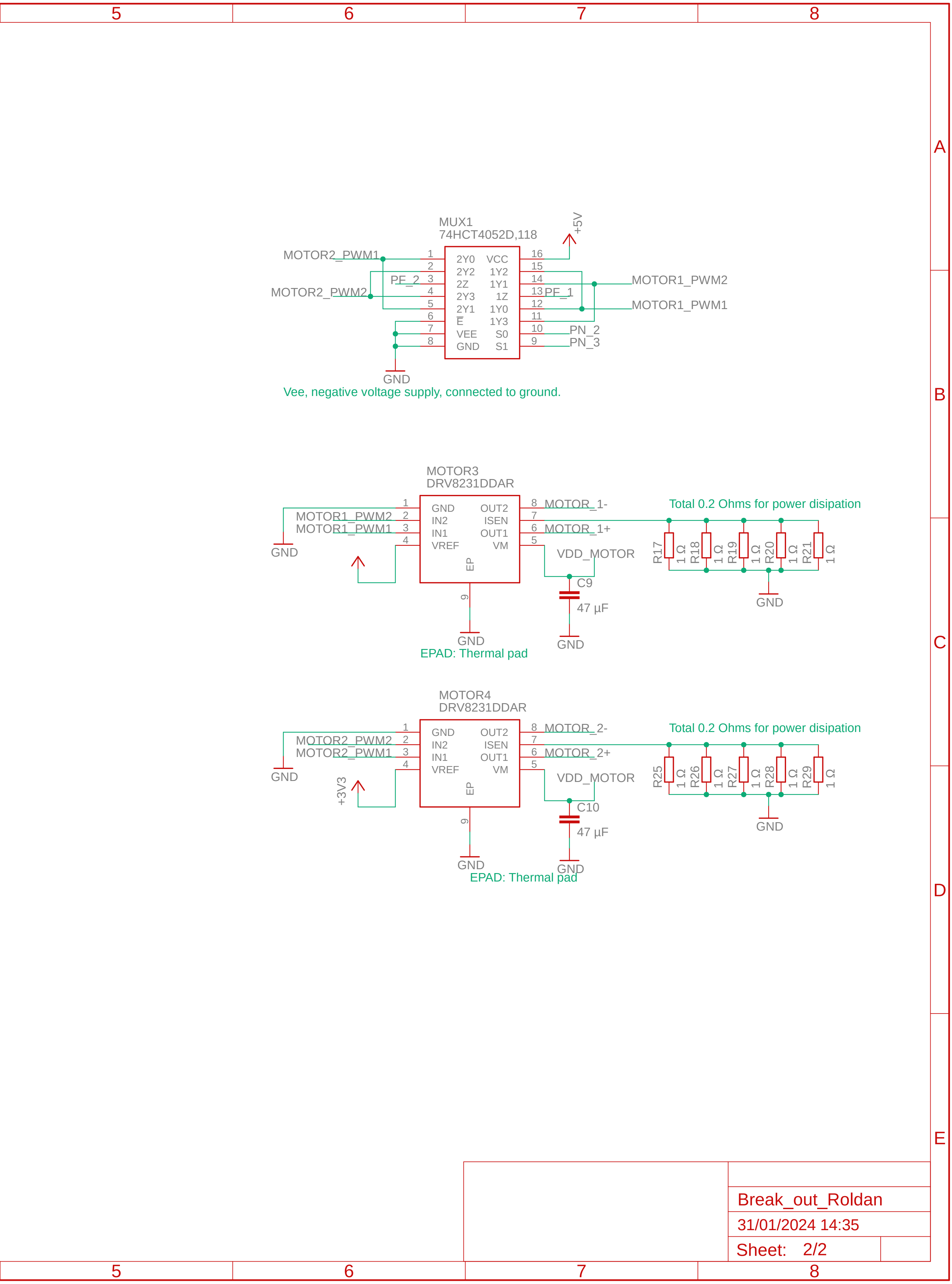

MUX1
74HCT4052D,118
+5V
MOTOR2_PWM1
MOTOR2_PWM2
PF_2
2Y0 VCC
2Y2 1Y2
2Z 1Y1
2Y3 1Z
2Y1 1Y0
E 1Y3
VEE S0
GND S1
PF_1
MOTOR1_PWM2
MOTOR1_PWM1
PN_2
PN_3
GND
Vee, negative voltage supply, connected to ground.
MOTOR3
DRV8231DDAR
GND OUT2
IN2 ISEN
IN1 OUT1
VREF VM
EP
MOTOR1_PWM2
MOTOR1_PWM1
MOTOR_1-
MOTOR_1+
VDD_MOTOR
C9
47 µF
Total 0.2 Ohms for power disipation
R17 1 Ω
R18 1 Ω
R19 1 Ω
R20 1 Ω
R21 1 Ω
GND
EPAD: Thermal pad
MOTOR4
DRV8231DDAR
MOTOR2_PWM2
MOTOR2_PWM1
+3V3
MOTOR_2-
MOTOR_2+
VDD_MOTOR
C10
47 µF
Total 0.2 Ohms for power disipation
R25 1 Ω
R26 1 Ω
R27 1 Ω
R28 1 Ω
R29 1 Ω
GND
EPAD: Thermal pad
Break_out_Roldan
31/01/2024 14:35
Sheet: 2/2

Declaration

I declare that this Bachelor Thesis has been completed by myself independently without outside help and only the defined sources and study aids were used.

[redacted]

City	Date	Signature